

Temp #77-59634

NASA CR-145104

**LOW-FREQUENCY NOISE REDUCTION OF  
LIGHTWEIGHT AIRFRAME STRUCTURES**

By

G.L. Getline

REPRODUCIBLE COPY  
ORIGINAL COPY

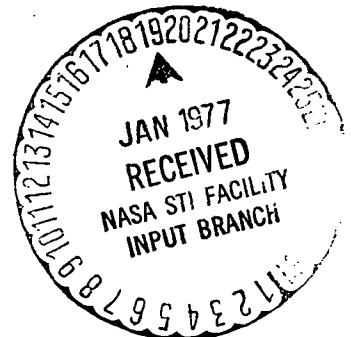
Prepared under Contract No. NAS1-13910

By

**GENERAL DYNAMICS CONVAIR DIVISION**  
San Diego, California

for

**NASA**  
National Aeronautics and  
Space Administration



**Page  
Intentionally  
Left Blank**



## TABLE OF CONTENTS

	Page
SUMMARY . . . . .	1
INTRODUCTION . . . . .	2
ANALYSES . . . . .	4
VIBRATION TESTS . . . . .	4
ACOUSTIC TESTS . . . . .	5
RESULTS AND DISCUSSION . . . . .	6
CONCLUSIONS . . . . .	8
RECOMMENDATIONS . . . . .	9
REFERENCES . . . . .	11
APPENDIX A - SUMMARY OF PANEL ANALYSES FOR DETERMINATION OF NATURAL FREQUENCIES	33
APPENDIX B DETAIL DRAWINGS OF TEST PANELS . . . . .	41
APPENDIX C VIBRATION TEST INSTRUMENTATION . . . . . AND PROCEDURES	51
APPENDIX D ACOUSTIC TEST CHAMBERS - INSTRU-. . . . . MENTATION AND PROCEDURES	53

Figure	LIST OF FIGURES	Page
1	Trend of Fuselage Sidewall Surface Densities . . . . .	13
2	Panel a,1, Al Frames, G/E Caps, Flat . . . . .	14
3	Panel b, Graphite Frames, Flat . . . . .	15
4	Panel e, Al Honeycomb, Flat . . . . .	16
5	Panel c, Graphite Frames, Curved . . . . .	17
6	Panel d, Graphite Corrugation, Curved . . . . .	18
7	Panel a, Transmission Loss . . . . .	20
8	Panel a,1, Transmission Loss . . . . .	21
9	Panel b, Transmission Loss . . . . .	22
10	Panel c, Transmission Loss . . . . .	23
11	Panel d, Transmission Loss . . . . .	24
12	Panel e, Transmission Loss . . . . .	25
13	Panel f, Transmission Loss . . . . .	26
14	Acoustic Transmission Loss - Mechanical Transmissibility . . . . .	27
15	Comparative Q's for Panel and Room Modes . . . . .	28
16	Transmission Loss Construction for Two Degrees-of-Freedom System . . . . .	29
17	Comparison of Construction from Figure 16 and TL Test Data from Figure 8 . . . . .	30
18	TL Curves for Panels with Room Effects Removed . . . . .	31
19	Noise Reduction for Panel b or c . . . . .	32
1A	Vibration Test Setup . . . . .	58
2A	Acoustic Test Setup . . . . .	59
3A	Vibration Test Setup . . . . .	61
4A	Anechoic and Reverberation Rooms . . . . .	62
5A	Instrumentation . . . . .	63
6A	Microphone Positions . . . . .	64
7A	Acoustic Test Setup (Reverberation Room Side). . . . .	65

## LIST OF FIGURES (Contd)

Figure		Page
8A	Acoustic Test Setup (Anechoic Room Side) . . . . .	66
9A	Standard Panel TL Calibration . . . . .	67
10A	Lumped Constant, K . . . . .	68

## LIST OF TABLES

Table		Page
1	76.2 × 101.6 cm (30 × 40) Inch Test Panels . . . . .	19
1A	Test Facilities and Instrumentation . . . . .	57
2A	Summation of Vibration Data . . . . .	60

## SUMMARY

Analytical and experimental studies of the noise signatures of various types of turbofan and propeller driven aircraft with power augmented lift systems, such as externally blown flaps, have shown that the noise is characterized by maximum intensity at low frequencies. Conventional type construction of aircraft cabins, which principally depends on structural weight as the basis for noise attenuation, cannot provide the reductions necessary to provide a tolerable acoustic environment for passengers. This report presents the results of an experimental study of the noise attenuation characteristics of aircraft-type fuselage structures constructed so as to provide high stiffness and low weight. Of particular significance and one of the main goals of the program was to determine both the feasibility and practicability of providing increased noise attenuation at low frequencies. Test data include the results of vibration and acoustic transmission loss tests on seven types of isotropic and orthotropically stiffened panels, both flat and curved, combining conventional aluminum alloy and high modulus-low density graphite/epoxy composites. All test panels were flightweight structure for transport type aircraft in the 34 050 to 45 400 kg (75,000 to 100,00 pound) gross weight range. The transmission loss data on the test panels, when converted to cabin noise reduction by applying available test data on the interior treatment of Convair 880 commercial jet transport aircraft, show that significant increases in noise reduction can be obtained (compared to the 880) at all frequencies below about 400 Hz, with essentially no degradation of noise reduction characteristics above 400 Hz. Because data in this study were obtained only on individual panels, recommendations are made for further work involving incorporation of stiffness-controlled cabin panels into an acoustically integrated aircraft cabin structure.

## INTRODUCTION

Acoustical treatments for the interiors of passenger carrying aircraft, whether today's large commercial jets or light propeller driven general aviation aircraft, have historically been added after the fact. That is, airframe structures are designed to carry required operational air and ground loads as efficiently as possible, and acoustical treatment typically in the form of fiberglass blankets, damping tape, etc. is added later. Further, since the weights of such materials are entirely parasitic, detracting from aircraft payload capability and performance, installation of these materials is under severe weight constraints. The net result of this situation is that cabin interior noise levels are often higher than desired, making speech communication difficult and accelerating physical fatigue.

The above situation has up to the present been tolerable, if not always acceptable. With the introduction of STOL aircraft using power augmented lift systems such as various types of blown flap arrangements, the after-the-fact approach for installation of interior acoustical treatment can no longer provide adequate noise reduction. There are several reasons for this. First, for aerodynamic reasons the engines of blown flap STOL aircraft are tucked in close to the fuselage. Thus, neglecting all other considerations, cabin noise levels of STOL aircraft have the potential for being on the order of 20 dB higher than in conventional (CTOL) jet aircraft. Second, the efficiency of a blown flap system in developing incremental lift is dependent on the span over which the jet is entrained. The use of special, high aspect ratio nozzles to increase the jet entrainment span, plus the spreading of the entrained jet itself causes a shift in the peak of the noise spectrum towards lower frequencies by an octave or more. Thus, the cabin noise problem in STOL aircraft is characterized by high noise levels at low frequencies, Reference 1. This type of environment is not generally amenable to alleviation by conventional aircraft acoustical treatments, which depend for the most part on structural weight and lightweight, fiberglass blankets. Further, incorporation of sufficient additional weight into the cabin walls for increased noise attenuation, whether added as structure or interior trim, would most likely be prohibitive.

However, there is another option for the achievement of high noise reduction at low frequencies, and that is by the use of "stiffness control." Most "standard" commercial aircraft cabin construction, that is, where the structure is designed by operational loads, tends to have major resonances (from the acoustical standpoint) in the 100-150 Hz range where noise due to powered lift augmentation may be a maximum. In addition to the structure providing low values of "mass law" transmission loss (TL) at these low frequencies, TL's decrease to nearly zero at the

resonances despite some alleviation by the addition of parasitic damping treatments to the structure. The term "stiffness control" implies the design of aircraft structure capable not only of carrying required operational loads but whose fundamental resonances are well above the frequency regime associated with maximum noise intensity. The requirement for high resonant frequencies defines a structure that is not only extremely stiff, but is also light. In short, there is described a structure whose load carrying and acoustical properties are integrated into a cohesive configuration for maximum efficiency.

It has been only fairly recently (for some of the reasons described above) that interest has developed in the aerospace industry with respect to the acoustic transmission properties of structures below their fundamental resonances. There has been some analytical work and a modicum of experimental work, mostly with models of various types, as described in References 2, 3, 4, 5, 6, 7, and 8, which are by no means exhaustive. Further, not all the work described in the references is directly applicable to the basic design problem under consideration; that is, the design of a large, lightweight, essentially cylindrical enclosure.

The work reported herein relates to the frequency regime where the ratio of fundamental structural resonant frequencies to fundamental acoustic resonances of the test facility is greater than 1.0. The test structures are all  $76.2 \times 101.6$  cm panels whose construction and surface density are within a practical range to allow design consideration for future STOL and CTOL aircraft. Designs embody both conventional aluminum alloy and graphite/epoxy composite construction. The intent was to obtain parametric information for a range of structural resonant frequencies in the form of acoustic transmission loss curves, from well below the fundamental resonances (stiffness-controlled regime) to well above resonance (mass-controlled regime). The full-scale frequency range which was investigated covers the center frequencies from 31.5 to 8000 Hz.

Initial design analyses of the test panels and preliminary vibration test data provide essentially uncoupled modes and resonant frequencies. Acoustic test data, however, provide acoustic-structural coupled modes because of the finite size of the test chamber. In addition to these basic data which are presented in this report, additional TL and NR curves are presented wherein the "room effects" have been removed, leaving only the structural characteristics. These "refined" data show that stiffness-control can provide effective, low-frequency noise reduction at acceptable structural weights. However, because the data presented herein was obtained on relatively small panels and was designed only to provide parametric information, recommendations are made for follow-on work to investigate the feasibility of applying this information to a full-scale aircraft cabin design with its attendant complexities related to dynamically matching the stiffness properties of

skins, ring frames and longitudinal stiffeners.

## ANALYSES

Limitations were set on the configurations of the  $76.2 \times 101.6$  cm test panels so that they would be representative of flightweight fuselage structures applicable to transport type aircraft in the 34 050 to 45 400 kg weight class. The trend in structural weight for a wide range of aircraft gross weights is shown in Figure 1. The test panels varied in surface density from 6.44 to 11.08 kg/m<sup>2</sup> (1.32 to 2.27 lbs/ft<sup>2</sup>) with an average density of 8.44 kg/m<sup>2</sup> (1.73 lbs/ft<sup>2</sup>).

Before establishing the design requirements for the test panels, room modes of the acoustic test facility were calculated. Fundamental volume resonances of both the reverberation and anechoic rooms of the acoustics laboratory, Figure 4A, were calculated to be about 80 Hz. Details of these calculations and experimental corroboration are contained in Appendix D. For this reason, in order to assure that the ratio of  $f_{11}$  (structural)/ $f_{111}$  (acoustical) would be significantly greater than 1.0, the minimum target panel design frequency was set at 200 Hz. Details of the panel analyses are contained in Appendix A; panel drawings are contained in Appendix B. Results of the preliminary vibration tests are contained in Appendix C. Differences between estimated and measured resonant frequencies are attributed mainly to the fact that the panels were analyzed as being simply supported, which was not attained when the actual panels were installed in the test frame, as shown in Figure 2A.

All test panels had a common aluminum alloy skin 1.524 mm (0.60 in) thick, with the exception of the honeycomb sandwich panels which had faces each 0.762 mm (0.030 in) thick for a total thickness of 1.524 mm (0.60 in). Stiffnesses and natural frequencies were varied by the types of construction, e.g., sheet-frame and honeycomb sandwich, and by application of low density - high modulus graphite/epoxy composites; also some panels were flat while others were curved, as described in Appendices A and B.

## VIBRATION TESTS

After fabrication, all panels were vibration tested to establish the resonant frequencies of major modes, with one exception. Panel a (Appendix A) was originally fabricated as Configuration a.1. After Panel a.1 had undergone vibration and acoustic transmission loss tests it was returned to the factory where the graphite/epoxy strips which had been scabbed onto the frames were removed, thus converting

it into Configuration a. By this time, however, the vibration test setup had been dismantled because of other laboratory commitments and it was not possible to accomplish a vibration survey on the re-worked panel.

The test panels are shown in Figures 2 through 6. The vibration test setup is shown in Figures 1A and 3A. Details of the test procedure and data are contained in Appendix C. The vibration tests were carried out under essentially free-space conditions and were required for two reasons. The first reason was that the frequencies estimated for design, rank-ordering purposes, were based on the assumption that the panels were simply supported and it was known that the actual restraints would be some combination of simply supported, clamped and free-free, as may be inferred from Figure 2A. Secondly, when undergoing transmission loss tests in the acoustics laboratory the effects of any acoustic-mechanical coupling between the test panels and the relatively small volumes of the reverberation and anechoic chambers could be isolated.

## ACOUSTIC TESTS

After completion of the vibration tests, the panels were moved to the acoustics laboratory for transmission loss tests. Before the panels were tested, both the reverberant and anechoic rooms were surveyed to determine room modes and frequencies, and also to determine the optimum locations for the TL microphones in both rooms.

A "standard" TL panel, 2.54 mm (0.1 inch) aluminum sheet, for which verified TL data were available was first re-calibrated to assure the adequacy of test procedures. Finally, all contract panels were tested. The data which were obtained were in the form of noise reduction (NR), facility related. These NR data were corrected to TL values by adjusting for the lumped parameters (K) of the facility obtained from previous "standard panel" tests conducted at Convair and Armour Research Laboratories.

Detail descriptions of the acoustic test facility, instrumentation and procedures are contained in Appendix D. This appendix also contains both the original and re-calibration data for the "standard panel," Figure 9A, and a plot of the lumped parameter for the facility (K) versus frequency, Figure 10A.



## RESULTS AND DISCUSSION

Table 1 summarizes the experimentally determined physical and dynamical properties of all the test panels. Detail descriptions are contained in Appendices A and B. It is noted that the fundamental resonant frequencies of the panels, as installed in the test fixture, meet the targeted design frequencies. Plots of acoustic transmission loss (TL) for the panels, as installed, are shown in Figures 7 through 13. It is noted that these basic plots represent data for the coupled, acousti-mechanical systems of the test chamber and panels and that the TL properties of the panels, per se, have not yet been isolated. The discussions in the following paragraphs relate to removal of the test chamber effects from the data, presentation of panel TL data (sans room effects) and commentary on the finalized data.

Considering a panel as a single degree-of-freedom system, that is, assuming that it can resonate only in its fundamental ( $f_{11}$ ) mode, an analogy between acoustic transmission loss and mechanical transmissibility of a single degree-of-freedom system can be established. If it is assumed that an oscillatory force (pressure) is directly applied to a lightly damped spring-mass system, then at frequencies an octave or more above resonance, the transmissibility may be expressed as  $T = 1/(\beta^2 - 1)$ , where  $\beta$  is the ratio of driving frequency to resonant frequency (Reference 9). By inspection it is noted as  $\beta$  becomes large, then  $T \approx 1/\beta^2$ . That is, the response of the mass is effectively inertial and decreases at 6 dB/octave as  $\beta$  increases; hence, "mass law." Below resonance, for a mechanical system, as  $\beta$  decreases,  $T = 1/(1 - \beta^2)$ . That is, at  $\beta = 0$ ,  $T = 1.0$ . (Note: Sign convention has been ignored for the sake of simplicity). This is only true, however, if the coupling efficiency between the driving force and the mass is maintained at all frequencies as, for example, by a rigid mechanical connection.

In the case of an oscillatory (acoustic) pressure acting on a panel, however, as the frequency of the pressure becomes lower the wavelength increases. As the wavelength become large with respect to the finite dimensions of the panel, coupling efficiency between the applied pressure and the panel decreases. At zero frequency, the wavelength is infinitely large and the coupling efficiency is zero. Thus, at zero frequency, or  $\beta = 0$ ,  $T = 0$ . For this system, then, below resonance  $T \approx \beta^2$ . The response is effectively a function of the stiffness of the system and decreases at 6 dB/octave as  $\beta$  decreases; hence, "stiffness control." If the transmissibility,  $T$ , is zero (at  $\beta = 0$  and  $\beta = \infty$ ) the panel must undergo no motion; hence its acoustic transmission loss must be infinitely large. At resonance, panel motion is controlled by its damping. The above discussion is illustrated by Figure 14, which is a plot of mechanical transmissibility ( $T$ ) and acoustic transmission loss (TL) for a panel with an arbitrarily selected resonant frequency of 400 Hz, and 2 percent critical

damping, excited by "white noise" and radiating into "free space."

If a panel comprised an element of the skin of an aircraft fuselage, the external side (on which noise is generated) would be exposed to free space. The internal side would be exposed to the interior volume of the cabin, which would have some nominal amount of acoustic absorption. The frequency for the coupled acousti-mechanical modes is derived in Reference 3. The equation as presented in Reference 8, is

$$\left(1 - \frac{\Omega^2}{\omega_{mn}^2}\right) \left(1 - \frac{\omega_m^2}{\Omega^2}\right)^{\frac{1}{2}} J'_n \left[ \frac{\Omega R}{c} \left(1 - \frac{\omega_m^2}{\Omega^2}\right)^{\frac{1}{2}} \right] + \frac{\rho c \Omega}{M_{\omega_{mn}}^2} J_n \left(1 - \frac{\omega_m^2}{\Omega^2}\right)^{\frac{1}{2}} = 0$$

where

$\Omega$  = frequency of coupled modes

$\omega_m$  = frequency of acoustic (organ pipe) modes

$M_{\omega_{mn}}^2$  = modal stiffness of fuselage shell

$R$  = shell radius

$\rho, c$  = density and speed of sound of interior volume

$J$  =  $n^{\text{th}}$  order Bessel function (prime denotes differentiation)

Considering Panel a.1, for example, with a surface density of 11.08 kg/m<sup>2</sup> (2.27 lbs/ft<sup>2</sup>) and a fundamental frequency of 500 Hz, it is seen that the ratio of the acoustic impedance of the air volume to the modal stiffness of the panel,  $\rho c / M_{\omega_{mn}}^2 = 3.81 \times 10^{-6}$ . That is, the ratio approaches zero. This essentially eliminates the last term in the above equation and yields the uncoupled frequencies of the room-panel system.

In the acoustic test facility, however, the noise is generated in a constrained volume (rather than in free space) and the transmitted noise (through the panel) is also measured in a constrained volume. At the resonant frequencies of the reverberation room, in which the noise is generated, there is large amplification of acoustic pressures. With an average absorption coefficient ( $\alpha$ ) of about 0.02 (Reference 10) across the frequency spectrum, the  $Q$  of the reverberation room at  $f_{221} = 125$  Hz, for example, is about 54.5 dB. Comparative  $Q$ 's for room and panel modes are shown in Figure 15. Again, at  $f_{221} = 125$  Hz, the amplified acoustic pressure in the reverberation room causes an amplified, driven response of the test panel, e.g.,

Panel a.1 which has its fundamental resonance at 500 Hz. This amplified, driven response of the test panel is evidenced by measurement of essentially uniform, non-modal sound pressure levels across the anechoic side of the panel determined by the use of fixed and roving microphones as described in Appendix D.

Because of the amplified panel response at the room resonant frequency, the TL of the panel decreases from the nominal value it would have at that frequency if the panel were not overdriven, just as if the panel itself were at resonance. Slightly below the room resonance there is an abrupt decrease in the acoustic driving pressure because of the very low damping (high Q), as shown in Figure 15. When this occurs the panel amplitude decreases, more slowly due to its higher damping, and the TL reverts to the level it would have had if the room resonance were nonexistent. Using actual values of Q from Figure 15 involving only two modes, i. e., Panel a.1 at 500 Hz and the 125 Hz room mode, and considering that excitation is provided by one-third octave band white noise; and further that the transmitted noise is measured through a one-third octave band filter which has a much greater bandwidth than either the room or panel, Reference 2, the following two degree-of-freedom construction is obtained as shown in Figure 16. A comparison between this construction and actual TL test data is shown in Figure 17. The agreement between the construction and actual test data is excellent around and below the resonant frequencies, considering that only one room mode and one panel mode were used in the construction. It is considered that the two curves would also coalesce in the high frequency regime if higher frequency room and panel modes were included in the construction. This demonstrates that reverberation room effects can be removed from the test data. Because the test panels were undamped, the high frequency TL's are strongly influenced by the high modal density at the high frequencies. It is considered that if these higher modes were damped, the TL curves would move towards the mass law idealization. Figure 18 shows a family of TL curves for the test panels, wherein room effects have been removed and it has been assumed that high frequency modes have been highly damped. Because the transmission loss concept does not apply to panels whose dimensions are smaller than one-half an acoustic wavelength, Reference 4, then at frequencies less than about 200 Hz (for the 30 x 40 inch test panels), the transmission loss (TL) must really be considered as de facto noise reduction (NR).

## CONCLUSIONS

1. When operating below the fundamental resonance of a structural panel, regardless of the panel surface density or the fundamental frequency, the slopes of all transmission loss (or noise reduction) curves must be parallel at -6 dB/octave.

2. For a given panel surface density, as its construction is varied in order to raise or lower its fundamental frequency, at any frequency an octave or more below resonance the transmission loss or noise reduction will increase with an increase in the fundamental frequency and will decrease with a decrease in that frequency.
3. For a given fundamental frequency of a panel, as the surface density is varied, the transmission loss or noise reduction at a given frequency below resonance will increase with surface density at 6 dB per weight doubling. This agrees with the theory of E. H. Dowell, Reference 16.
4. To obtain the maximum noise reduction across the total frequency spectrum, the structural configuration should be designed to optimize the tradeoff between maximizing the fundamental frequency and maximizing its weight including added damping treatment. Additional weight in the form of absorptive blankets and interior trim which will provide added noise reduction should be isolated from the structure insofar as is practicable.
5. As shown in Figure 19, a stiffness controlled-acoustically integrated structure can provide very high noise reductions at low frequencies, without significantly affecting its high frequency noise reduction capability.

## RECOMMENDATIONS

It is recommended that, in order to resolve design problems related to the inter-relationship between skin, frame and longitudinal members of a full-scale aircraft cabin and to demonstrate the feasibility of constructing such a cabin with a stiffness controlled-acoustically integrated structure, that the following work be undertaken:

1. Carry out a detail design study for the cabin of specific category of aircraft (or other aerospace vehicle) where the acoustic problems are known and where loads and limiting structural weights can be precisely defined. This study should provide a flight weight and flightworthy structural concept.
2. Fabricate a full-scale segment of the aircraft cabin according to the results of the above design study. This segment should have a minimum length which includes at least five major frames.
3. Conduct vibration tests on the cabin segment to validate attainment of stiffness goals. During this test program any deficiencies should be corrected by progressively incorporating design changes into the structure. Vibration tests

should then be re-run on the modified structure. This procedure should be repeated as required to obtain the optimum acoustically integrated structure within program guidelines.

4. Conduct acoustic noise reduction tests on the optimized cabin structure in a reverberant environment with progressively applied interior treatment to demonstrate achievable noise reduction re required reduction.
5. Finally, demonstrate noise reduction and interior noise levels of the fully treated cabin segment when exposed to the noise generated by actual propulsion and powered lift systems.

## REFERENCES

1. "Proceedings of Conference on Powered-Lift Aerodynamics and Acoustics;" NASA Langley Research Center, May 24-26, 1976.
2. "Methods of Flight Vehicle Noise Prediction;" P. A. Franken and E. M. Kerwin, et al; WADC TR 58-343, November 1958.
3. "Structural-Acoustic Response, Noise Transmission Losses and Interior Noise Levels of an Aircraft Fuselage Excited by Random Pressure Fields;" J. A. Cockburn and A. C. Jolly; AFFDL-TR-68-2, August 1968.
4. "Low-Frequency Noise Reduction of Spacecraft Structures;" R. H. Lyon, et al, NASA CR-589, September 1966.
5. "Noise Reduction of Rectangular Enclosures With One Flexible Wall;" R. H. Lyon; JASA Vol. 35, No. 11, November 1963.
6. "Current Developments in Interior Noise and Sonic Fatigue Research;" G. Sengupta, Boeing Commercial Airplane Co., Seattle, Washington.
7. "Attenuation of Low Frequency Noise by a Stiffness Controlled Airframe Structure;" G. L. Getline, General Dynamics/Convair, CASD-ERR-73-050, December 1973.
8. "Prediction of Light Aircraft Interior Noise;" J. T. Howlett and D. A. Morales, NASA TMX-72838, April 1976.
9. "Mechanical Vibrations;" J. P. Den Hartog; McGraw-Hill Book Co., Inc.
10. "Acoustics;" L. L. Beranek; McGraw-Hill Book Co., Inc., 1954.
11. "Sound Absorption Coefficients of Architectural Acoustical Materials;" Acoustical Materials Association, Bulletin XIX.
12. "Sonic Fatigue Design Guide for Military Aircraft;" F. F. Rudder, Jr. and H. E. Plumblee, Jr.; AFFDL-TR-74-112, May 1975.
13. "Honeycomb Sandwich Design;" Hexcel Products, Inc.

14. "Acoustic Survey of Bldg 68, Ramp, San Diego;" Convair Report 66-2-M-75-27,  
Dated 3 July 1975.
15. "Summary and Interpretation of Panel Sound Transmission Loss Measurements;"  
Convair Report AG22-005, June 1958.
16. "A Primer for Structural Response to Random Pressure Fluctuations,"  
Dowell and Vaicaitis; Princeton University AMS Report 1220, 1975.

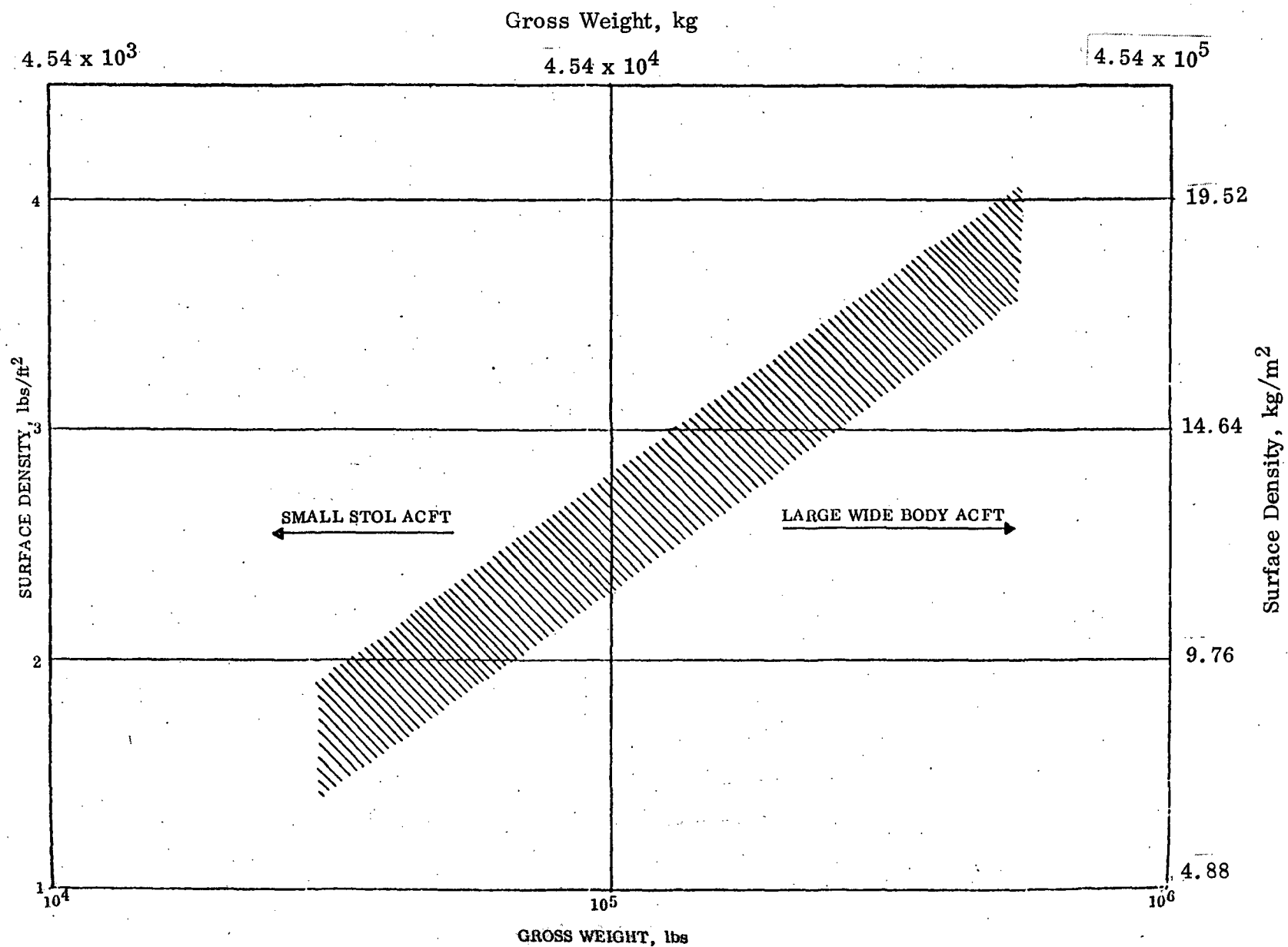


Figure 1. Trend of Fuselage Sidewall Average Surface Density for Transport Category Aircraft





Figure 2. Panel a.1 - 10.16 cm (4.0 in) Aluminum Frames, G/E Caps Flat

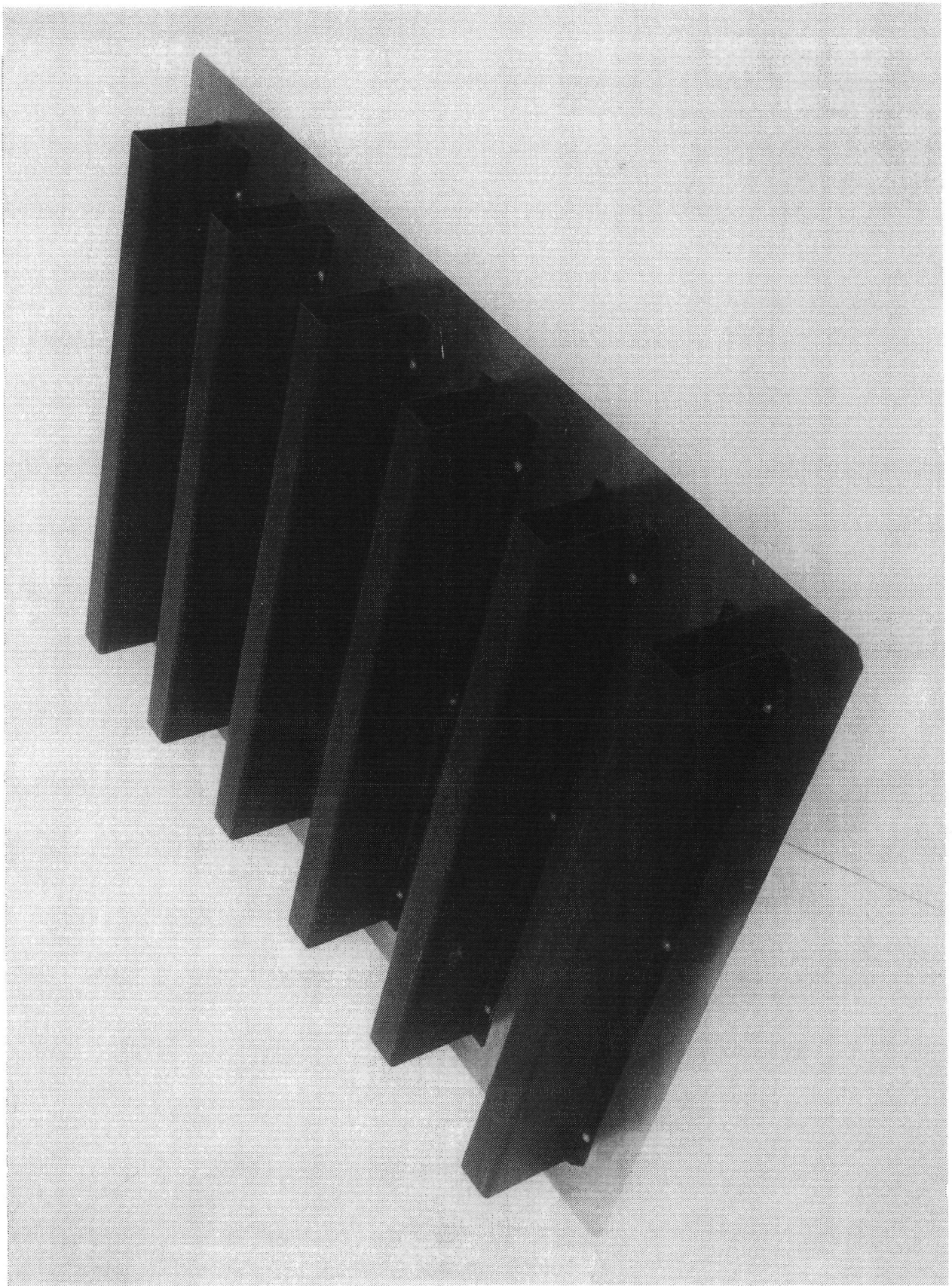


Figure 3. Panel b - 10.16 cm (4.0 in) Graphite Frames - Flat



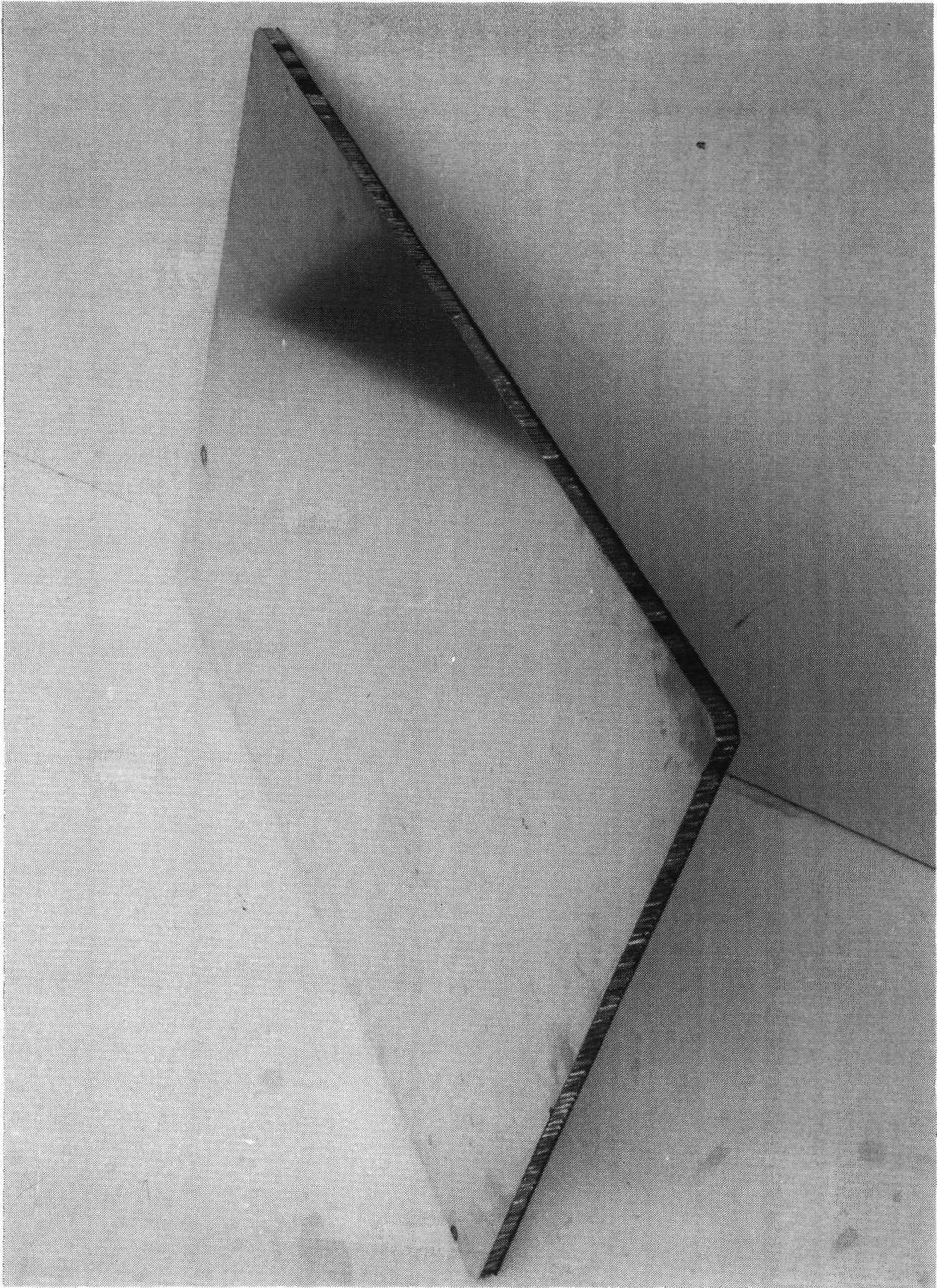


Figure 4. Panel e - Honeycomb - Flat

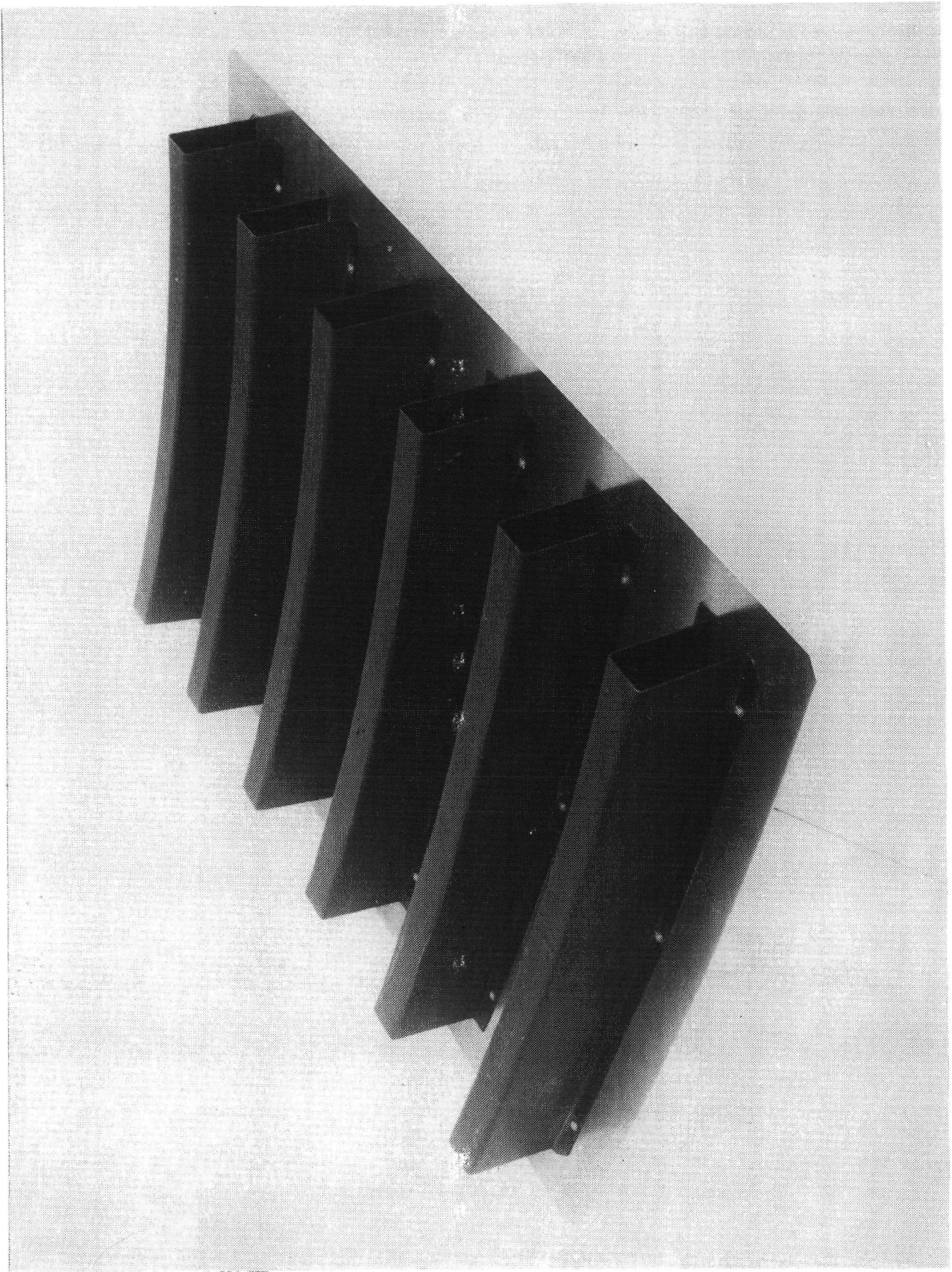


Figure 5. Panel c, 10.16 cm (4.0 in) Graphite Frames - Curved



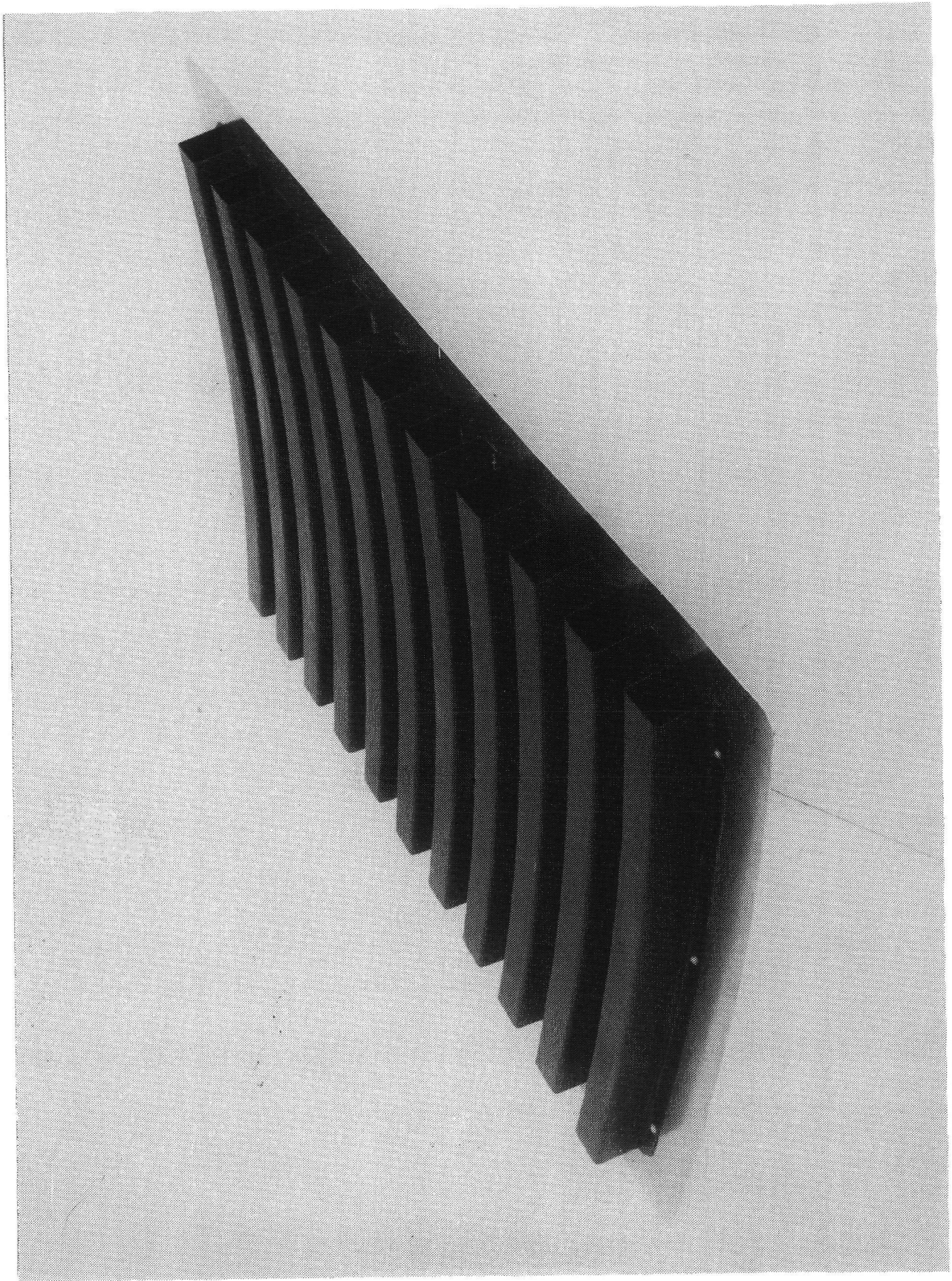


Figure 6. Panel d - 5.08 cm (2.0 in) Graphite Corrugation - Curved

Table 1. 76.2 × 101.6 cm (30 × 40 inch) Test Panels

Panel No.	Description (Note: All frames are along 76.2 cm Dimensions)	Surface Density kg/m <sup>2</sup>	f <sub>11</sub> Hz	c/c <sub>c</sub> *
a	Flat, 1.524 mm al skin, 10.16 cm deep al hat frames at 16.56 cm spacing	10.74	410 est.	.020 est.
a.1	Same as a, but also has 0.762 mm graphite/epoxy strips on al frame caps	11.08	500	.020
b	Same as a, except frames <b>all</b> graphite/epoxy	8.00	820	.018
c	Same as b, except panel has 317.5 cm radius of curvature along 76.2 cm dimension	8.00	815	.005
d	317.5 cm radius along 0.762 mm dimension, 1.524 mm al skin, 5.08 cm deep graphite/epoxy corrugations at 8.26 cm spacing	8.30	465	.013
e	Flat, al honeycomb sandwich, 19.05 mm thick core, 0.762 mm faces	6.44	225	.040
f	Same as e, except panel has 317.5 cm radius of curvature along 76.2 cm dimension	6.44	420	.022

\*c/c<sub>c</sub> obtained from half-power frequencies during vibration frequency sweeps at 2 min. octave.

ADD 4.9 DB TO OBTAIN OCTAVE BAND LEVEL

THIRD-OCTAVE BAND TRANSMISSION LOSS - dB

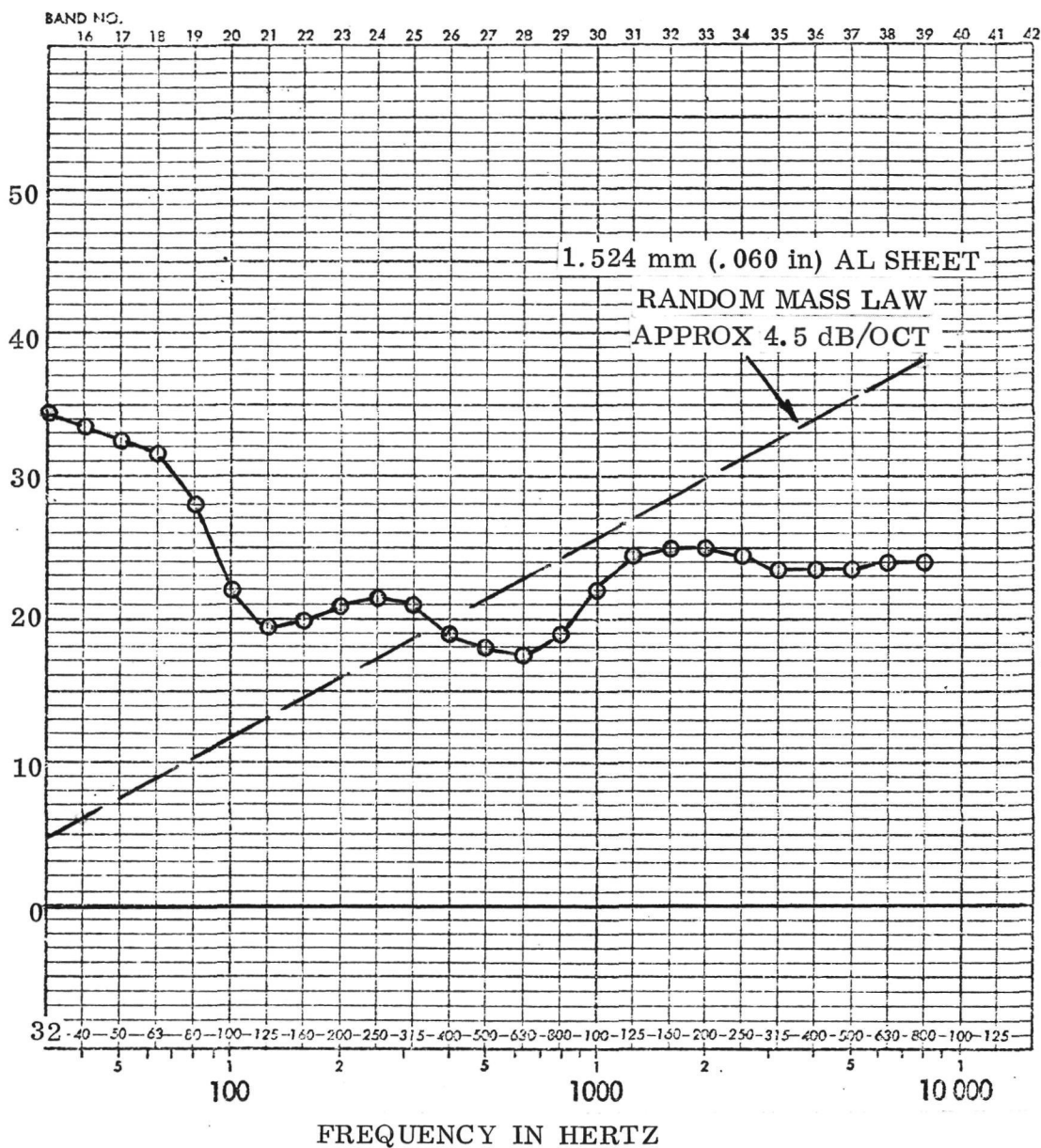


Figure 7. Panel a - Flat, 1.524 mm (.060 in) Al Skin, 10.16 cm (4 in) Deep Al Hat Frames on 16.94 cm (6.67 in) Centers

ADD 4.9 DB TO OBTAIN OCTAVE BAND LEVEL

THIRD-OCTAVE BAND TRANSMISSION LOSS - dB

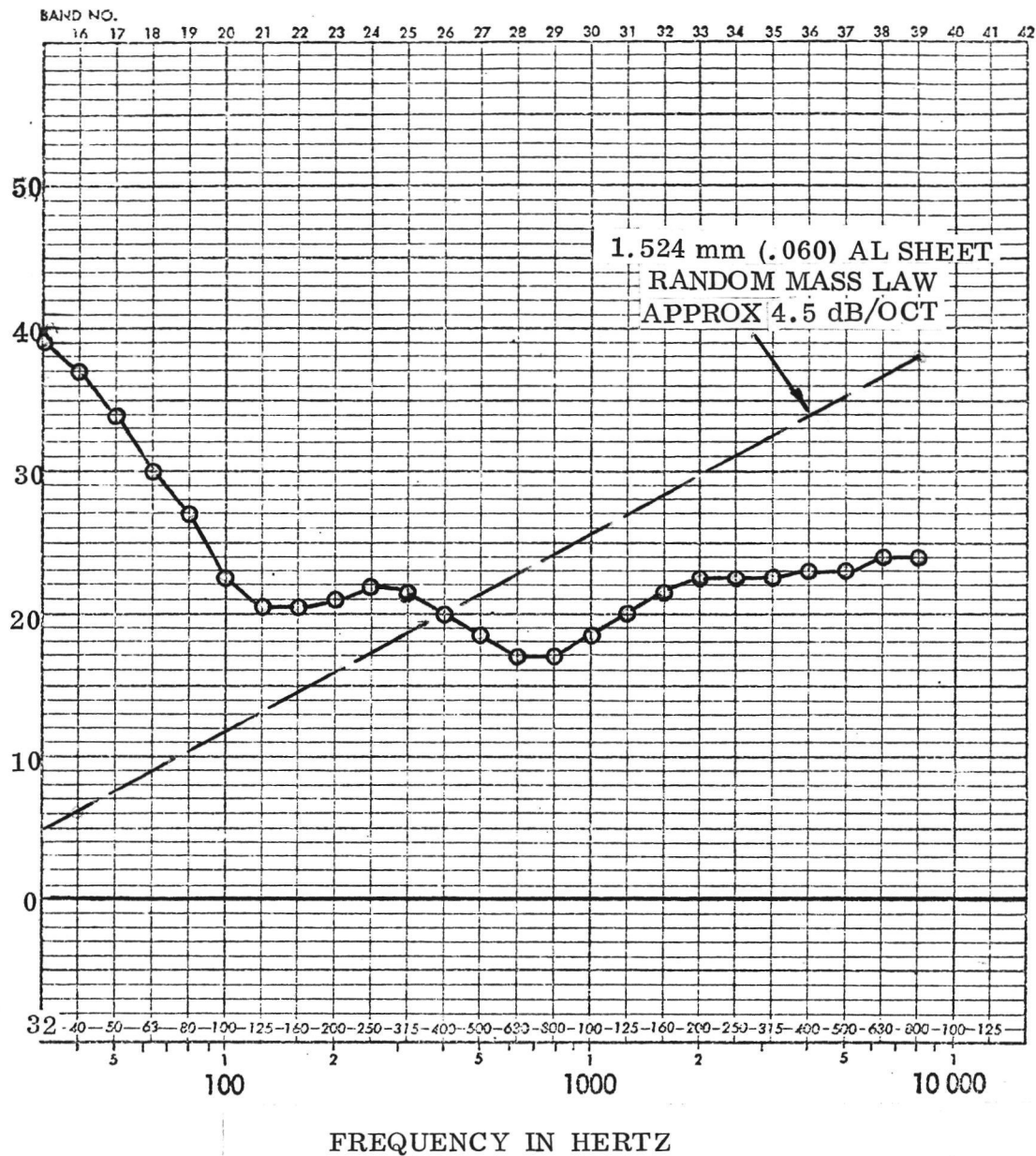


Figure 8. Panel a.1, Flat, 1.524 mm (.060 in) Al Skin,  
10.16 cm (4 in) Deep Al Hat Frames With  
Graphite/Epoxy Caps, on 16.94 cm (6.67 in)  
Centers





ADD 4.9 DB TO OBTAIN OCTAVE BAND LEVEL

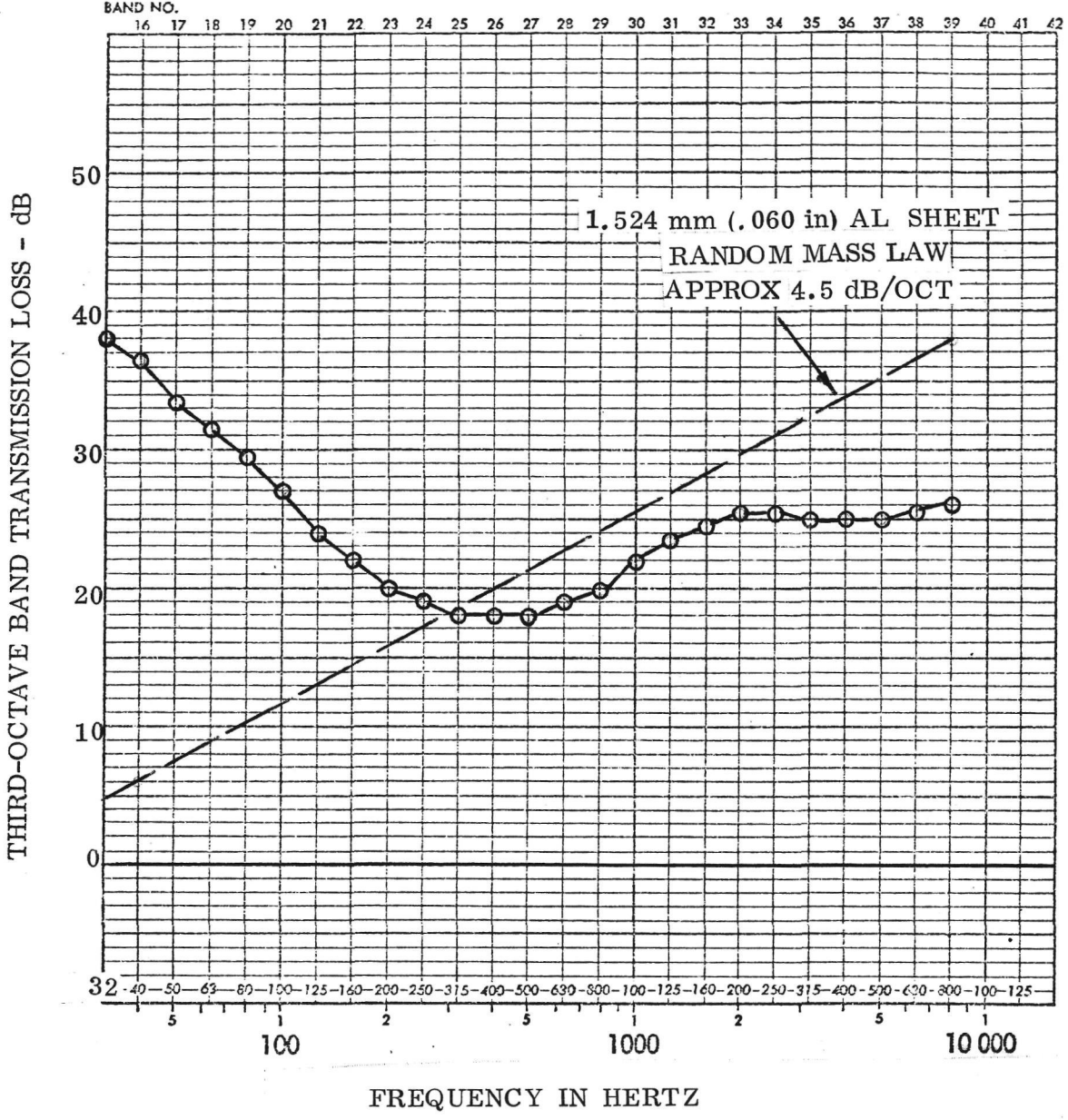


Figure 9. Panel b., Flat, 1.524 mm (.060 in) Al Skin, 10.16 (4 in)  
Deep Graphite/Epoxy Hat Frames on 1.694 cm (6.67 in) Centers



ADD 4.9 DB TO OBTAIN OCTAVE BAND LEVEL

THIRD-OCTAVE BAND TRANSMISSION LOSS - dB

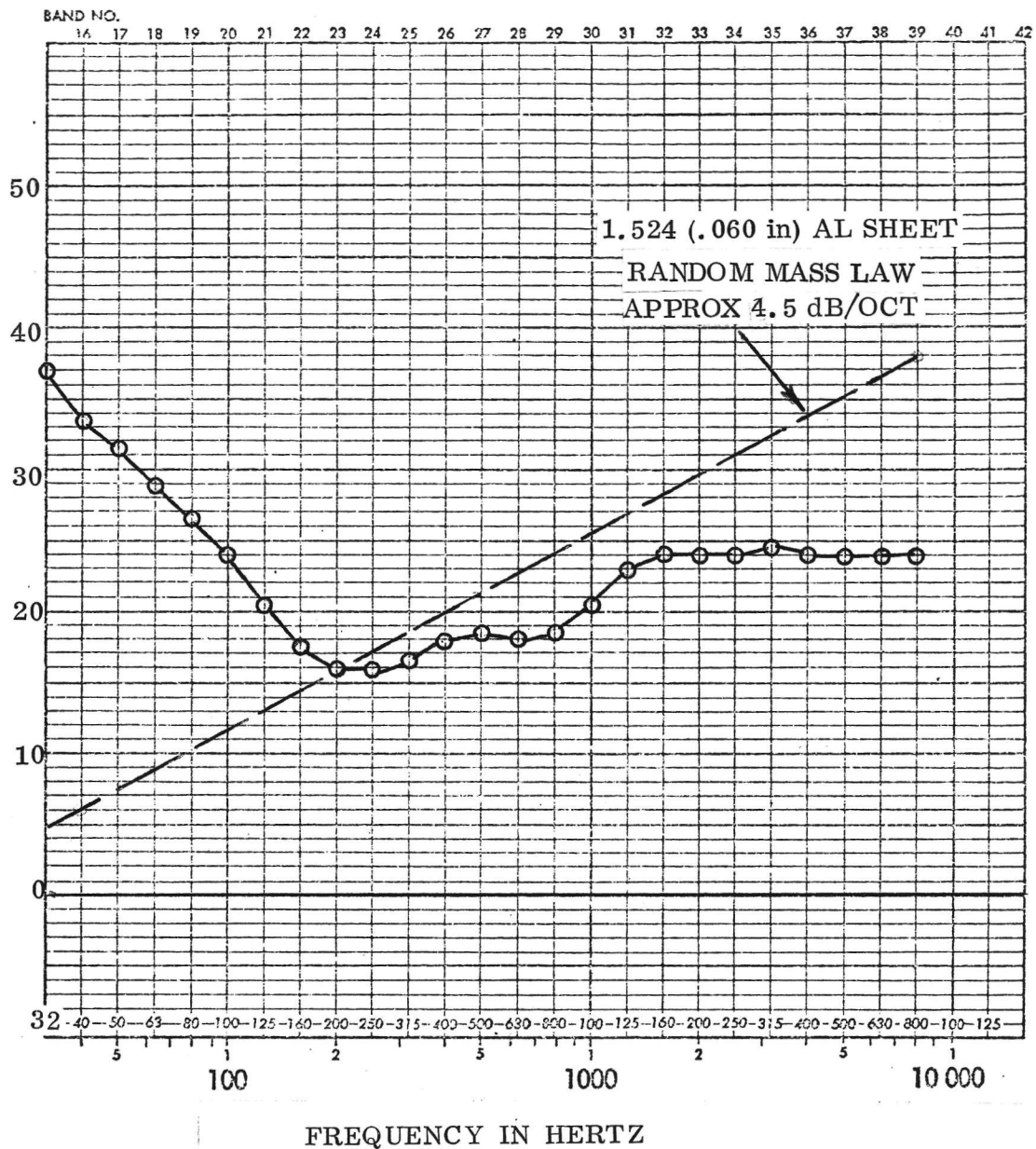


Figure 10. Panel c, 317.5 cm (125 in) Radius Curvature, 1.524 mm (.060 in) Al Skin, 10.16 cm (4 in) Deep Graphite/Epoxy Hat Frames on 16.94 cm (6.67 in) Centers

ADD 4.9 DB TO OBTAIN OCTAVE BAND LEVEL

THIRD-OCTAVE BAND TRANSMISSION LOSS - dB

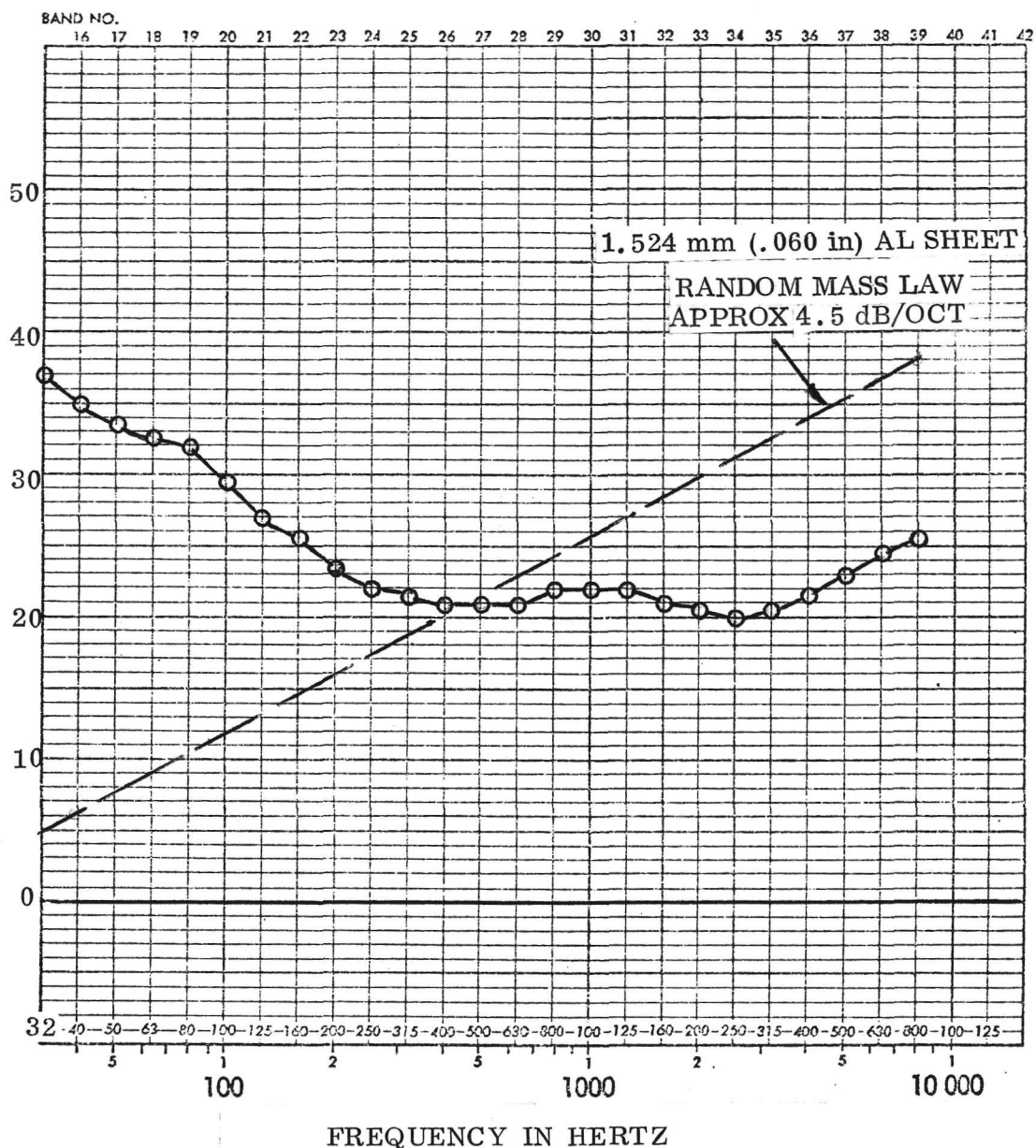


Figure 11. Panel d, 317.5 cm (125 in) Radius Curvature, 1.524 mm (.060 in) Al Skin, 5.08 cm (2 in) Deep  $\times$  4.45 cm (1.75 in) Wide Graphite/Epoxy Corrugations on 6.35 cm (2.50 in) Centers



ADD 4.9 DB TO OBTAIN OCTAVE BAND LEVEL

THIRD-OCTAVE BAND TRANSMISSION LOSS - dB

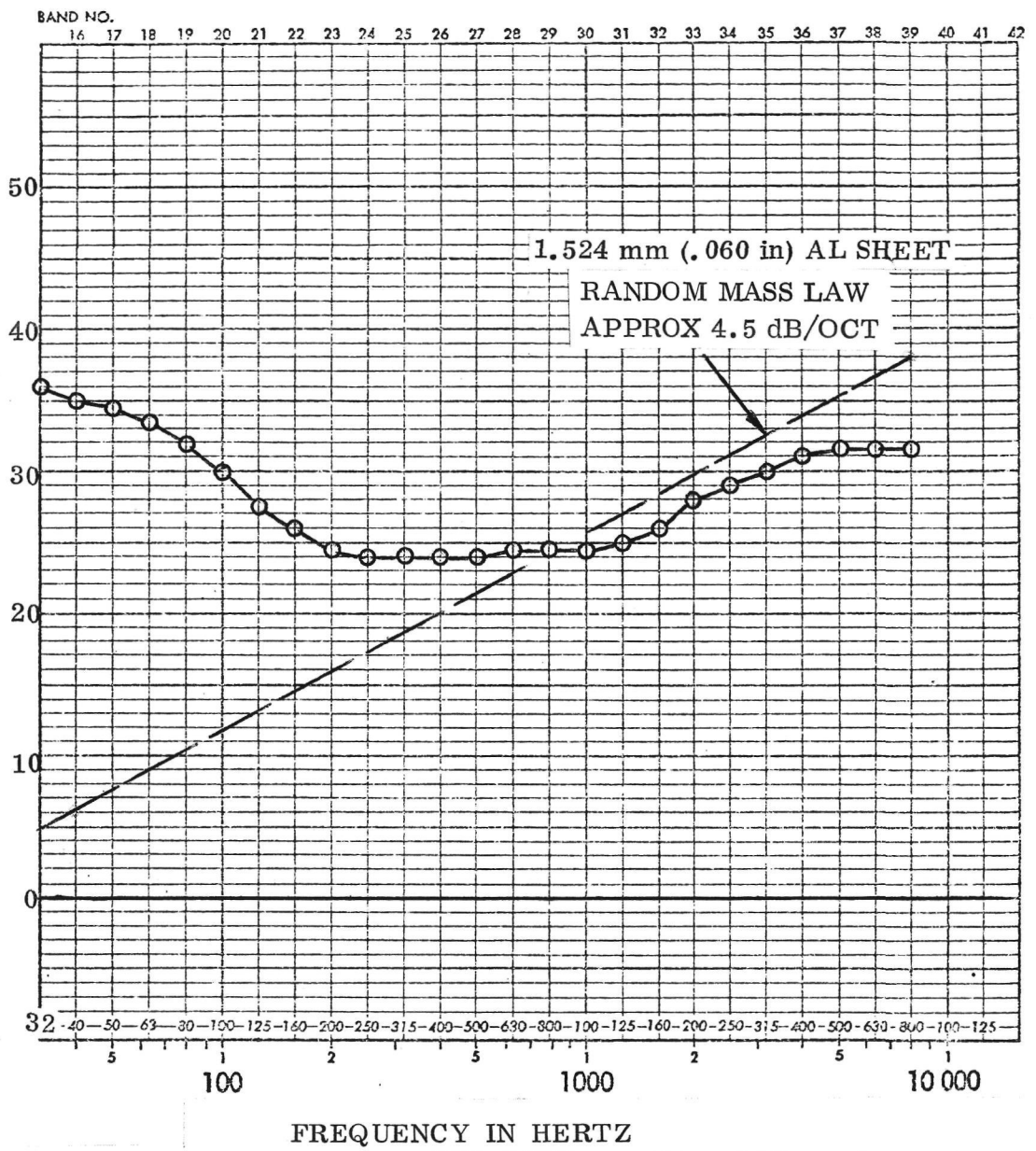


Figure 12. Panel e, Flat, Al Alloy Honeycomb Sandwich, 19.05 mm (0.75 in) Thick With 0.762 mm (.030 in) Al Faces

ADD 4.9 DB TO OBTAIN OCTAVE BAND LEVEL

THIRD-OCTAVE BAND TRANSMISSION LOSS - dB

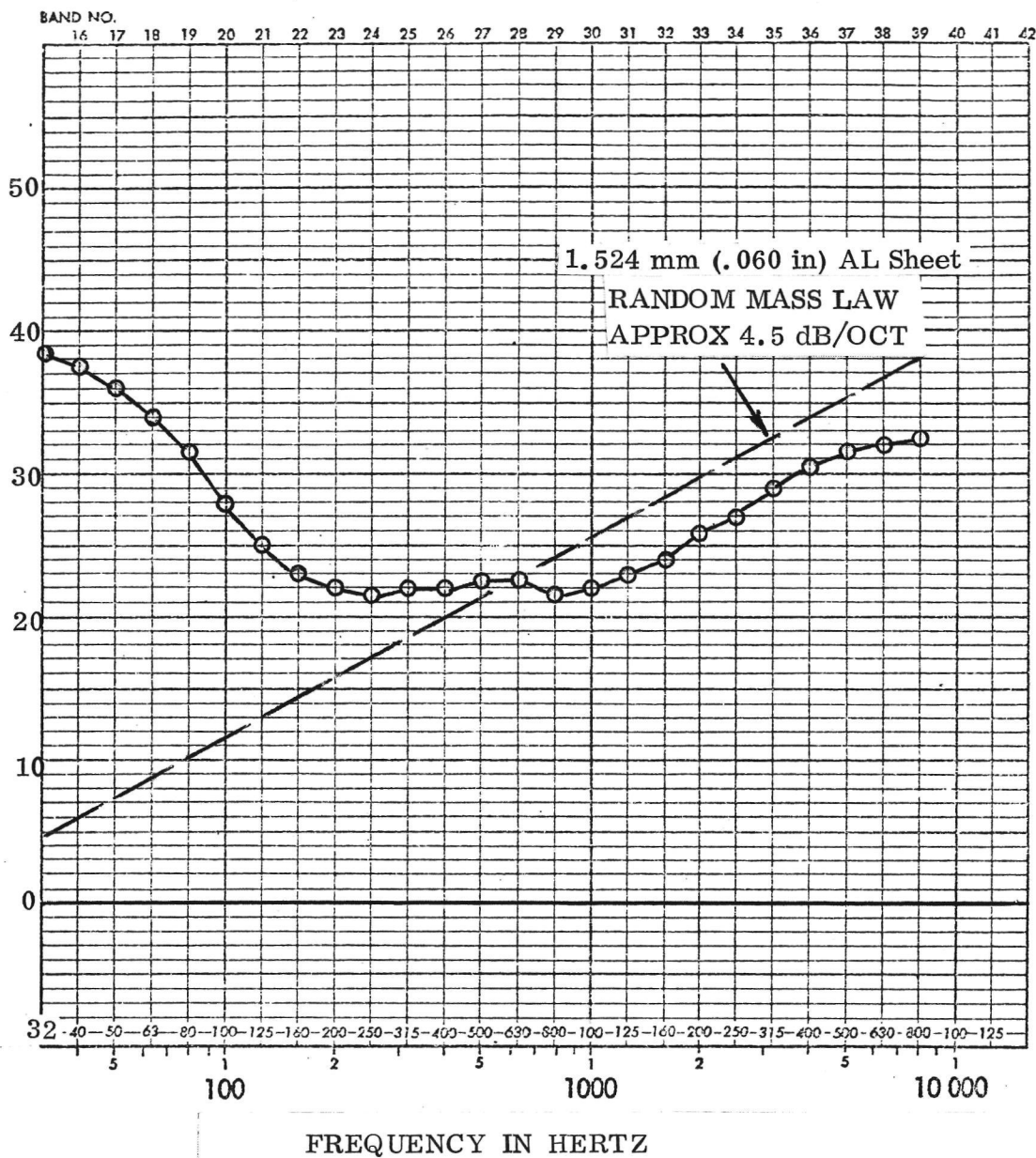


Figure 13. Panel f, 317.5 cm (125 in) Radius Curvature Al Alloy Honeycomb Sandwich 19.05 mm (0.75 in) Thick With 0.762 mm (.030 in) Al Faces



ADD 4.9 DB TO OBTAIN OCTAVE BAND LEVEL

THIRD-OCTAVE BAND TRANSMISSION LOSS - dB

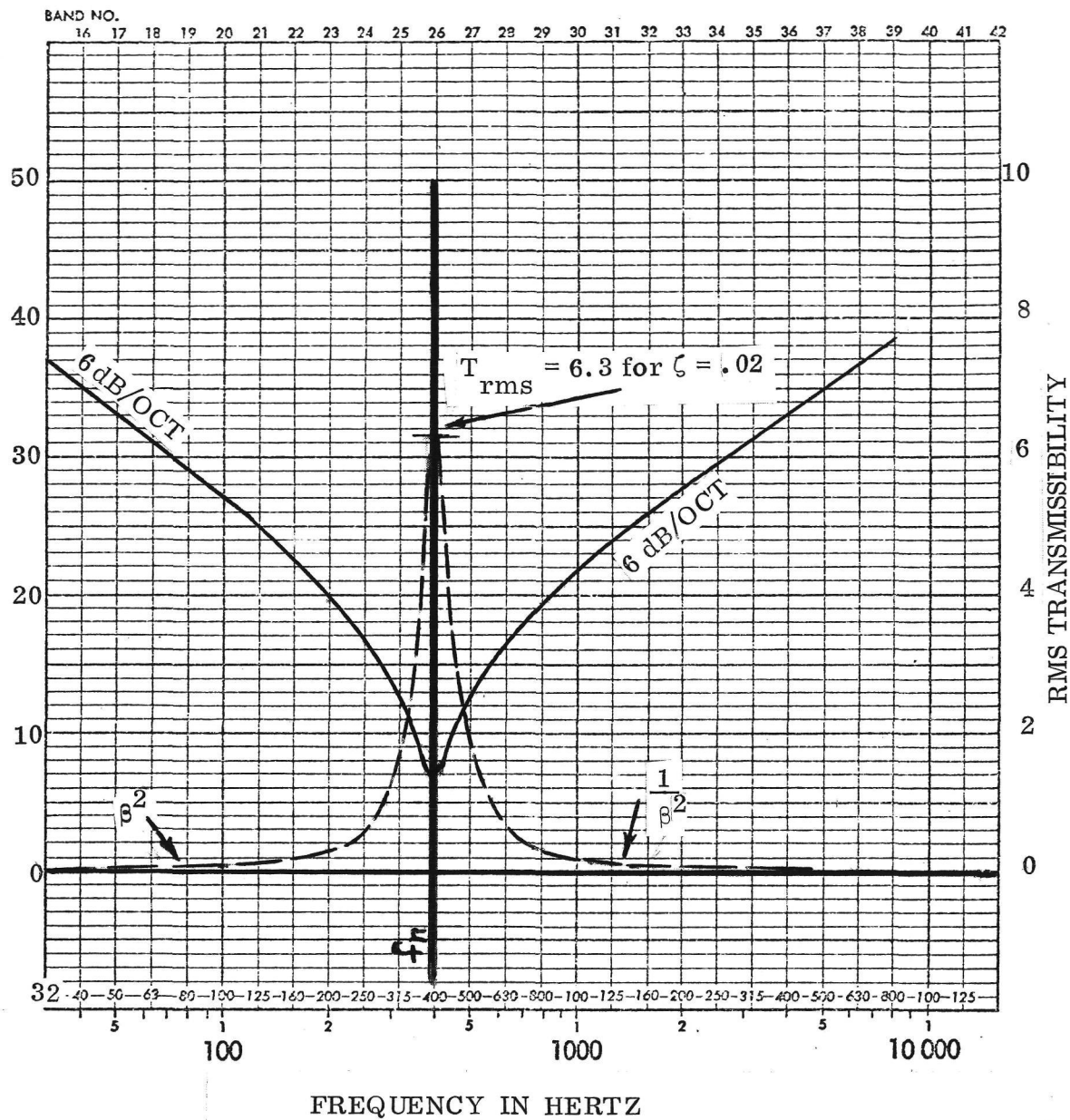


Figure 14. Relationship Between **Acoustic** Transmission Loss and Mechanical Transmissibility for a **Single** Degree-of-Freedom System

ADD 4.9 DB TO OBTAIN OCTAVE BAND LEVEL

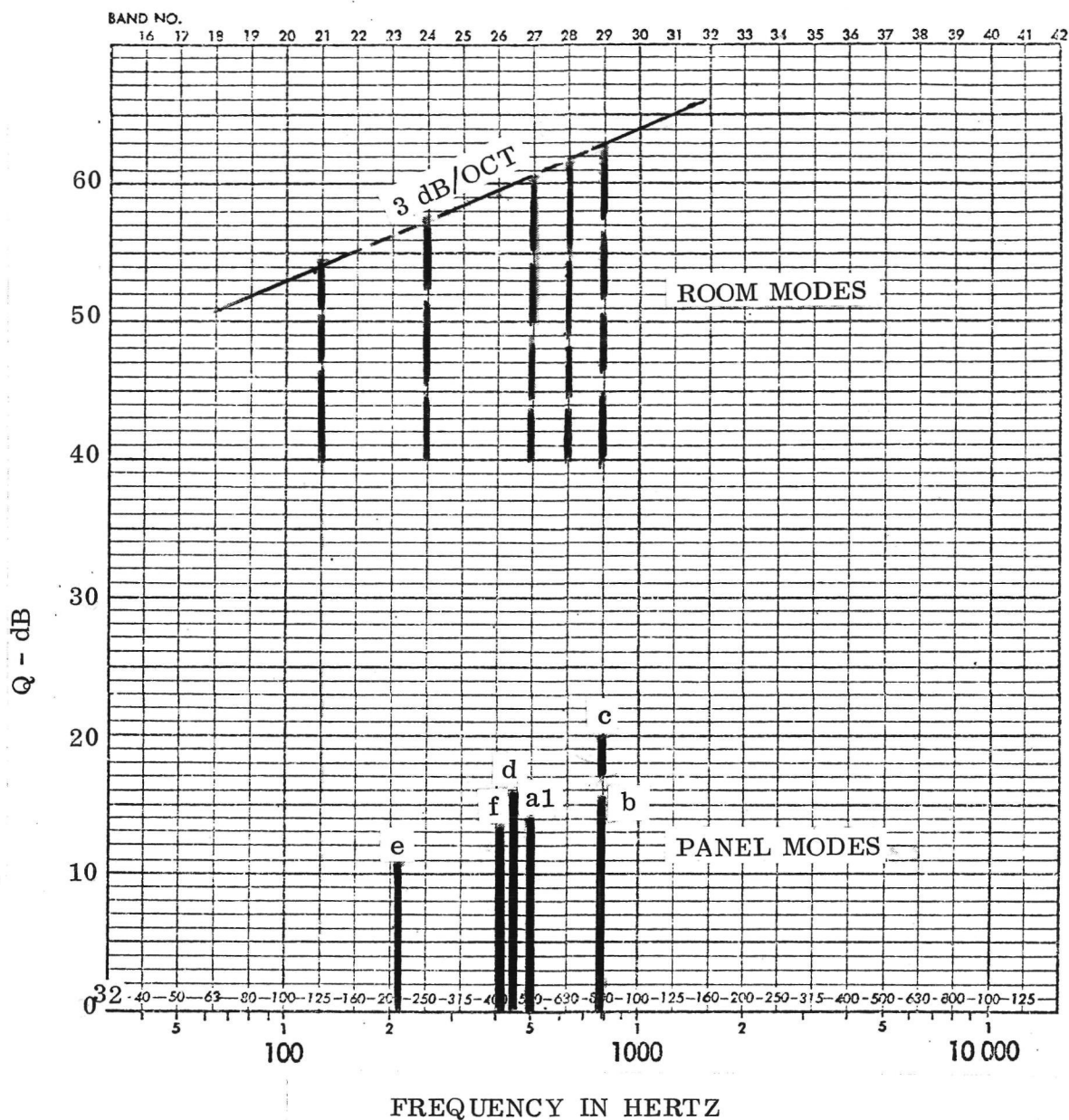


Figure 15. Comparative Dynamic Magnification at Resonance (Q) for Panel and Significant Room Modes

ADD 4.9 DB TO OBTAIN OCTAVE BAND LEVEL

THIRD-OCTAVE BAND TRANSMISSION LOSS - dB

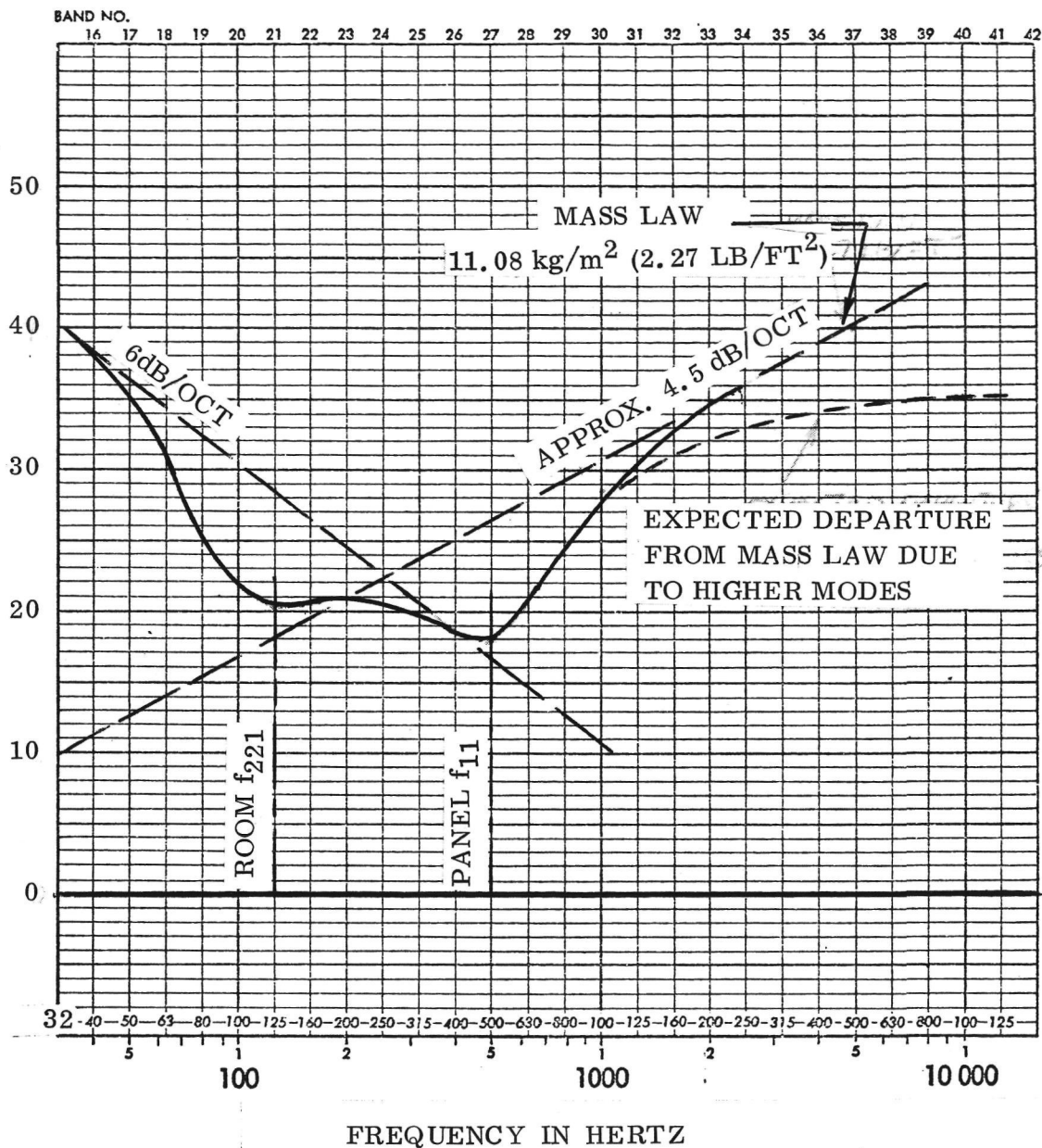


Figure 16. Transmission Loss Construction for Two Degree-of-Freedom System Utilizing Only Surface Density of Panel a. 1, Damping, and  $f_{11} = 500$  Hz; and Room  $f_{221} = 125$  Hz and Damping



### ADD 4.9 DB TO OBTAIN OCTAVE BAND LEVEL

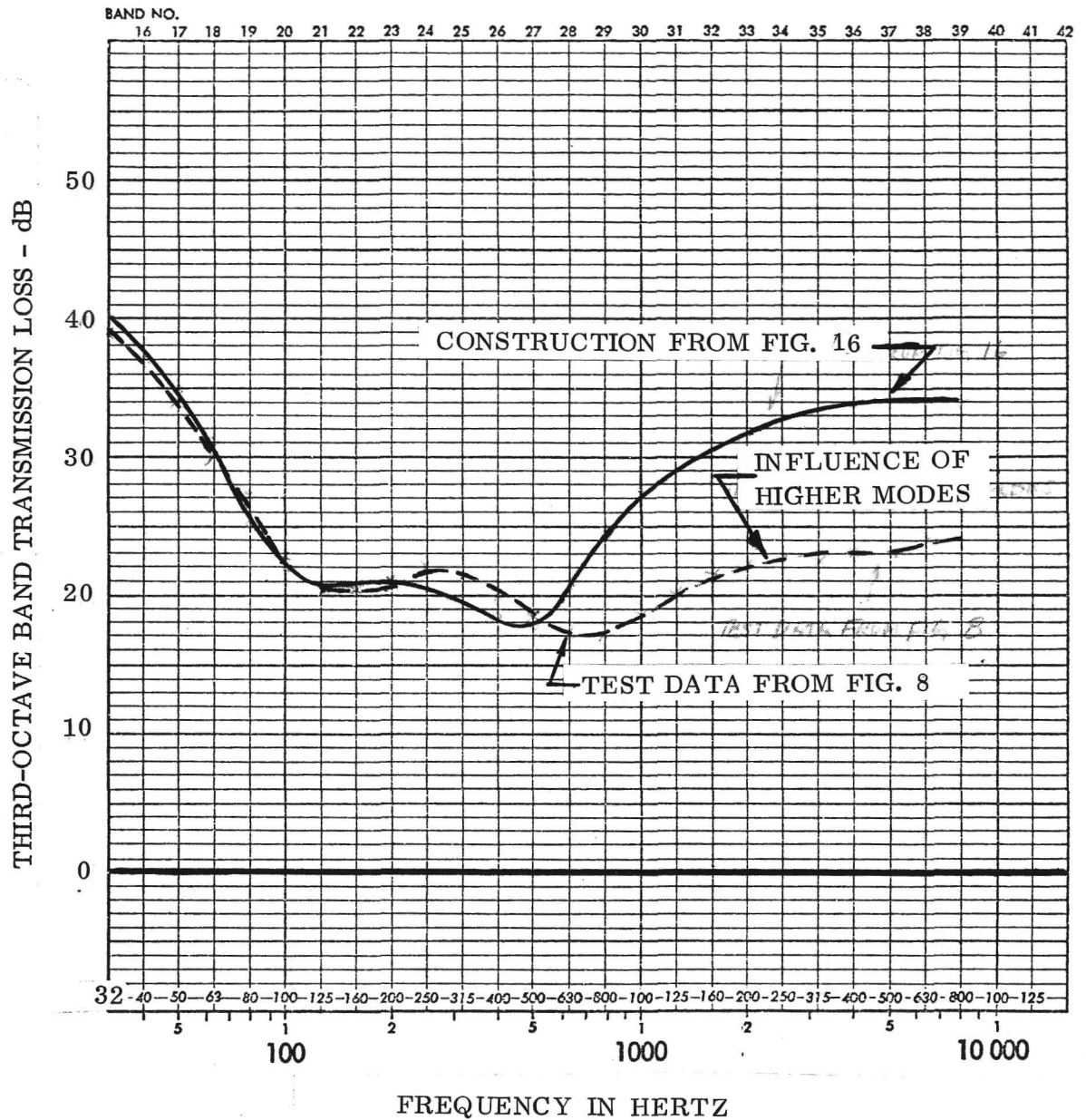


Figure-17. Panel a.1, Comparison Between Two Degree-of-Freedom Construction From Figure 16 and Actual TL Test Data From Figure 8

ADD 4.9 DB TO OBTAIN OCTAVE BAND LEVEL

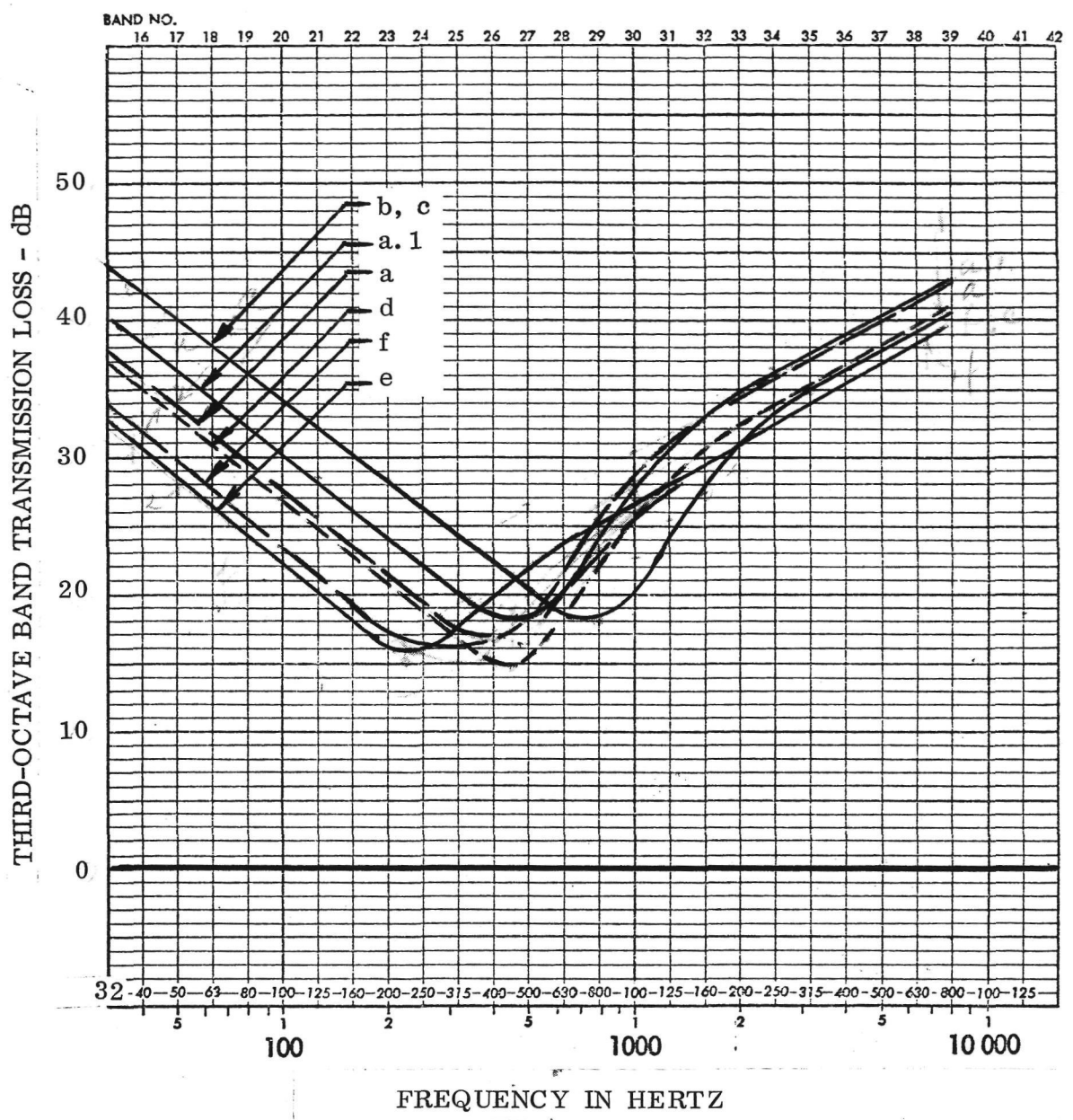


Figure 18. Transmission Loss Curves For Test Panels With Room Effects Removed and all Resonances Above Fundamental Assumed Highly Damped



ADD 4.9 DB TO OBTAIN OCTAVE BAND LEVEL

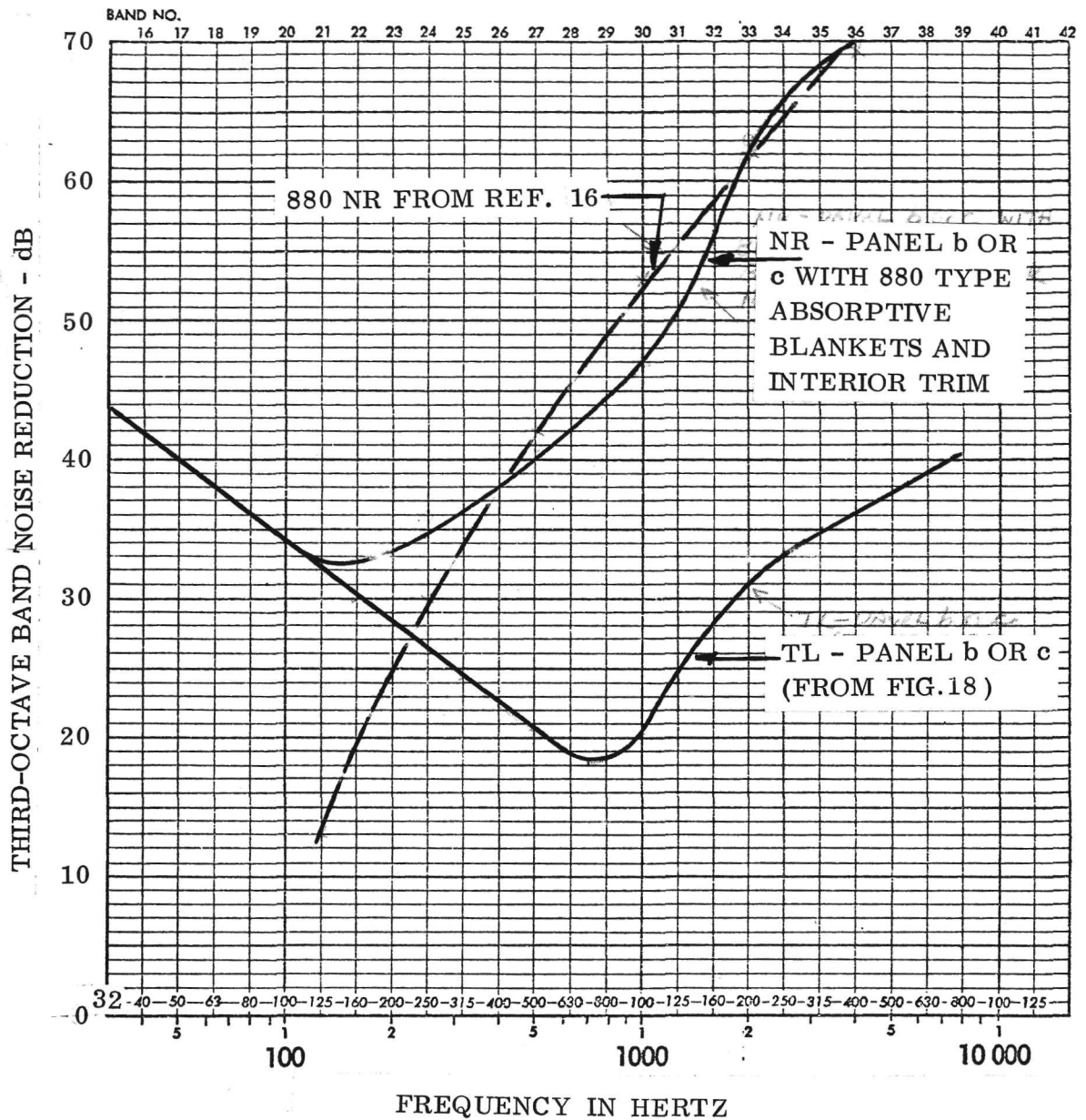


Figure 19. Noise Reduction Obtained by Panel b or c (Figure 18) With 880 Jet Transport Type Interior Trim - Isolated From Structure

## APPENDIX A

### SUMMARY OF PANEL ANALYSES FOR DETERMINATION OF NATURAL FREQUENCIES

NOTE: Panels are nominally 30x40 inches and are as noted in Paragraph 2 of the contractual statement of work, and as detailed in Paragraph 3 of Monthly Progress Report No. 1, T-SC-5-01, dated 9 July 1975. Analyses assume panels are simply supported. Dimensions are in lb-in. units. For conversion to metric units, see page 39.

Panel a: A1. alloy, flat sheet - frame construction (Ref. Dwg. No. 72C0546, Appendix B).

Actual wt = 18.3 lbs; surface density =  $2.20 \text{ lbs/ft}^2$ . Based on al. alloy density =  $0.1 \text{ lb/in}^3$ , surface density of 0.060 sheet =  $0.006 \text{ lb/in}^2$ . (Note: All panel skins are 0.060 inch thick).

Let  $M$  = skin mass surface density =  $0.006/386 = 1.554 \times 10^{-5} \text{ lb sec}^2/\text{in}^3$

$D$  = skin flexural rigidity =  $Eh^3/12(1-\sigma^2)$ , where

$E$  = Young's modulus,  $\text{lbs/in}^2$

$h$  = skin thickness, inches

$\sigma$  = Poisson's ratio

$D = 197.8 \text{ lb in.}$

For an orthotropic, stiffened panel, let  $D_x$  and  $D_y$  be the flexural rigidities along the X (about Y) and along the Y (about X) axes. The stiffeners provide little additional rigidity along the X (about Y) axis. Thus,  $D_x = D = 197.8 \text{ lb in.}$  and  $D_y = D + (EI_x/a)$  (flexural rigidity per unit panel width) where  $I_x/a$  is the running moment of inertia of the stiffeners.

$I_x/a = 0.221 \text{ in}^4/\text{in}$ , and

$D_y = 197.8 + 10^7 \times 0.221 \approx 2.21 \times 10^6 \text{ lb in.}$

Let  $k_m$  and  $k_n$  be panel wave numbers in X and Y directions, where m and n are the mode numbers, i.e., number of 1/2 wavelengths. For the fundamental mode, m and n = 1.

$$k_m = m\pi/40, \text{ and } k_n = n\pi/30$$

$$k_m = \pi/40, \text{ and } k_n = \pi/30 \text{ for } m = n = 1$$

The total flexural stiffness of the structure is, then,

$$K_T = \left[ (D_x)^{1/2} k_m^2 + (D_y)^{1/2} k_n^2 \right]^2 \quad (\text{Reference 11})$$

For the fundamental mode,

$$K_T = \left[ (197.8)^{1/2} (\pi/40)^2 + (2.21 \times 10^6)^{1/2} (\pi/30)^2 \right]^2$$

$$K_T = 268.4 \text{ (lb/in)/in}^2$$

The total panel surface density (est.) =  $0.014 \text{ lbs/in}^2$ ;

$$\text{Mass Density} = 3.627 \times 10^{-5} \text{ lb sec}^2/\text{in}^3$$

$$\omega_{11} = (268.4/3.627 \times 10^{-5})^{1/2} = 2720 \text{ rad/sec}$$

$$f_{11} = 433 \text{ Hz (est)}$$

Note: The panel as fabricated had six stiffeners rather than five, as originally conceived. Thus,  $D_y = 6/5 \times 2.21 \times 10^6 = 2.652 \times 10^6 \text{ lb in.}$   
(Thus  $K_T = 322 \text{ (lb/in)/in}^2$ .)

$$\omega_{11} = 2980 \text{ rad/sec}$$

$$*f_{11} = 474 \text{ Hz (final est)}$$

Panel a, 1: Same as Panel a, except that graphite/epoxy composite material is scabbed onto cap of stiffeners. G/E thickness - 0.030 in. (Ref. Dwg. No. 72C0546, Appendix B).

M Modulus of G/E,  $E = 2.5 \times 10^7$  lbs/in<sup>2</sup>  
 Density of G/E = 0.06 lbs/in<sup>3</sup>

As calculated for Panel a,

$$\begin{aligned} D_x &= 197.8 \text{ lb in.} \\ D_y &= 4.06 \times 10^6 \text{ lb in.} \\ K_T &= 492 \text{ (lb/in)/in}^2 \\ M_T &= 3.731 \times 10^{-5} \text{ lb sec}^2/\text{in}^3 \\ \omega_{11} &= (492/3.73 \times 10^{-5})^{1/2} = 3631 \text{ rad/sec.} \\ *f_{11} &= 578 \text{ Hz (est).} \end{aligned}$$

Panel b: Same as Panel a, except that frames are all graphite/epoxy construction.  
 (Ref. Dwg. No. 72C0546, Appendix B). As before,

$$\begin{aligned} D_x &= 197.8 \text{ lb in.} \\ D_y &= 5.525 \times 10^6 \text{ lb in.} \\ K_T &= 668.4 \text{ (lb/in)/in}^2 \\ M_T &= 2.85 \times 10^{-5} \text{ lb sec}^2/\text{in}^3 \\ \omega_{11} &= (668.4/2.85 \times 10^{-5})^{1/2} = 4843 \text{ rad/sec.} \\ f_{11} &= 770 \text{ Hz (est)} \end{aligned}$$

Correcting for six frames,

$$*f_{11} = 843 \text{ Hz (est)}$$

Panel c: Same as Panel b, except that panel has single curvature (R=125 inches) along major axis of frames. (Ref. Dwg. 72C0547, Appendix B). The following equation shows that the frequency of a curved panel is the frequency of a flat panel plus the curvature effect. Thus,

$$f_{11}^2 \text{ (curved)} = f_{11}^2 \text{ (flat)} + \frac{Em^4}{4\pi^2 \rho R^2 [m^2 + n^2 (a/b)^2]^2} \text{ (simply supported)}$$

For the fundamental,

$$f_{11}^2 \text{ (curved)} = f_{11}^2 \text{ (flat)} + \frac{E}{4\pi^2 \rho R^2 [1 + (a/b)^2]^2} \quad \text{(Reference 12)}$$

where,  $\rho$  = mass density and  $m$ ,  $n$ ,  $a$  and  $b$  are as before. First, consider an isotropic panel between frames,

$$f_{11} \text{ (flat)} = 329 \text{ Hz}$$

$$f_{11}^2 \text{ (curved)} = 329^2 + \frac{(2.5 \times 10^7)(386)}{4\pi^2 \times 0.1 \times 125^2 [1 + (4.17/30)^2]^2}$$

$$f_{11}^2 \text{ (curved)} = 108,241 + 120,572$$

$$*f_{11} \text{ (curved)} = 478 \text{ Hz}$$

Next, consider the complete orthotropic panel, (Note: The nominal value of  $E$  is pro-rated on the basis of the moments of inertia of aluminum alloy and graphite/epoxy elements. The nominal value of  $\rho$  is pro-rated on the basis of the volumes of aluminum alloy and graphite/epoxy). Hence,

$$\text{Nominal } E = 2.065 \times 10^7 \text{ lbs/in}^2$$

$$\text{Nominal } \rho = 1.99 \times 10^{-4} \text{ lb sec}^2/\text{in}^4$$

$$f_{11}^2 \text{ (curved)} = 770^2 + \frac{2.065 \times 10^7}{4\pi^2 \times 1.99 \times 10^{-4} [1 + (40/30)^2]^2 \times 125^2}$$

$$f_{11}^2 \text{ (curved)} = 592,900 + 21,802 = 614,702$$

$$*f_{11} \text{ (curved)} = 784 \text{ Hz (est)}$$

Correcting for six frames,

$$*f_{11} \text{ (curved)} = 859 \text{ Hz (est)}$$

Note: It appears that if an orthotropic panel is very stiff to start with, shallow curvature does not significantly increase its stiffness, e.g., from 843 Hz (flat) to 859 Hz (curved). However, the stiffness of the single isotropic bays between frames is greatly increased, e.g., from 329 Hz (flat) to 478 Hz (curved).

Panel d: Aluminum alloy curved skin (R= 125 in.) with stiffening provided by uni-directional, graphite/epoxy corrugations, (Ref. Dwg. No. 72C05417, Appendix B).

Note: If pure flexure is considered and all torsion neglected, the overall flexural stiffness of the built-up panel can be taken as merely the effect of the flat panel plus the corrugation stiffnesses placed in parallel. This assumption is generally only applicable to the fundamental mode where all the stiffening corrugations can be assumed to be in flexure.

$$D_x = 197.8 \text{ lb in. (as before)}$$

$$D_y = 3.55 \times 10^6 \text{ lb in.}$$

The total flexural stiffness of the flat orthotropic panel is, then,

$$K_T \left[ (197.8)^{1/2} (\pi/40)^2 + (3.55 \times 10^6)^{1/2} (\pi/30)^2 \right]^2$$

$$K_T = 430.18 \text{ (lb/in)/in}^2$$

$$M_T = 3.94 \times 10^{-5} \text{ lb sec}^2/\text{in}^3$$

$$\omega_{11} = (430.18/3.94 \times 10^{-5})^{1/2} = 3,304 \text{ rad/sec.}$$



$$f_{11} = 526 \text{ Hz (flat panel, est)}$$

Now, including the effects of curvature as before,

$$\text{Nominal } E = 2.08 \times 10^7 \text{ lb/in}^2$$

$$\text{Nominal } \rho = 1.844 \times 10^{-4} \text{ lb sec}^2/\text{in}^4$$

$$f_{11}^2 \text{ (curved)} = 526^2 + \frac{2.08 \times 10^7}{4\pi^2 \times 1.844 \times 10^{-4} \times 125^2 [1 + (40/30)^2]^2}$$

$$*f_{11} \text{ (curved)} = 548 \text{ Hz (est)}$$

Panel e: Aluminum alloy flat honeycomb sandwich construction; panel-no frames.

(Ref. Dwg. No. 72C0544, Appendix B).

$$\text{Core Density} = 4.5 \text{ lbs/ft}^3 = 0.0026 \text{ lbs/in}^3$$

$$\text{Core thickness, } t_c = 0.75 \text{ in.}$$

$$\text{Both facing sheets, } t_f = 0.030 \text{ inch; density} = 0.1 \text{ lb/in}^3$$

Panel flexural rigidity,

$$D = \frac{E t_f t_c t_f}{1.82}, \text{ where } t = \text{total thickness of sandwich}$$

$$D = \frac{10^7 \times 0.030 \times 0.75 \times 0.81}{1.82} = 1.00 \times 10^5 \text{ lb in. (Reference 13)}$$

Surface density of sandwich,

$$w = (0.0026)(0.75) + (2)(0.030)(0.1) = 0.00795 \text{ lb/in}^2 = 1.15 \text{ lb/ft}^2$$

Mass per unit area,

$$M = 0.00795/386 = 2.06 \times 10^{-5} \text{ lb sec}^2/\text{in}^3$$

$$f_{11} = \frac{K}{2\pi a^2 (M/D)^{1/2}}, \text{ where } K \text{ relates to } b/a = 40/30$$

$$f_{11} = \frac{14.88}{2\pi \times 30^2 \left[ (2.06 \times 10^{-5}) / (1 \times 10^5) \right]^{1/2}} \quad (\text{Reference 4})$$

$$*f_{11} = 183 \text{ Hz (est)}$$

Panel f: Same as Panel e, except for single curvature with R = 125 inches.  
(Ref. Dwg. No. 72C0545). Panel density,  $\rho = (2.06 \times 10^{-5}) / 0.81 = 2.54 \times 10^{-5} \text{ lb sec}^2 / \text{in}^2$ .

As before,

$$f_{11}^2 (\text{curved}) = 183^2 + \frac{10^7}{4\pi \times 2.54 \times 10^{-5} \times 125^2 \left[ 1 + (40/30)^2 \right]^2}$$

$$f_{11}^2 (\text{curved}) = 33,489 + 82,716 = 116,205$$

$$*f_{11} (\text{curved}) = 341 \text{ Hz (est).}$$

#### Conversion Factors - English to Metric Units

<u>Multiply</u>	<u>By</u>	<u>To obtain</u>
Pounds (wt)	0.454	kilograms (kg)
pounds/foot <sup>2</sup> (Surface density)	4.882	kilogram/metre <sup>2</sup> (kg/m <sup>2</sup> )
inches	2.54	centimetres (cm)
inches	2.54	millimetres (mm)

**"Page missing from available version"**

" page 40 "

## APPENDIX B

### DETAIL DRAWINGS OF TEST PANELS

Dwg. No. 72C0544; Panel-Test, Honeycomb Core, Flat

Dwg. No. 72C0545; Panel-Test, Honeycomb Core, Curved

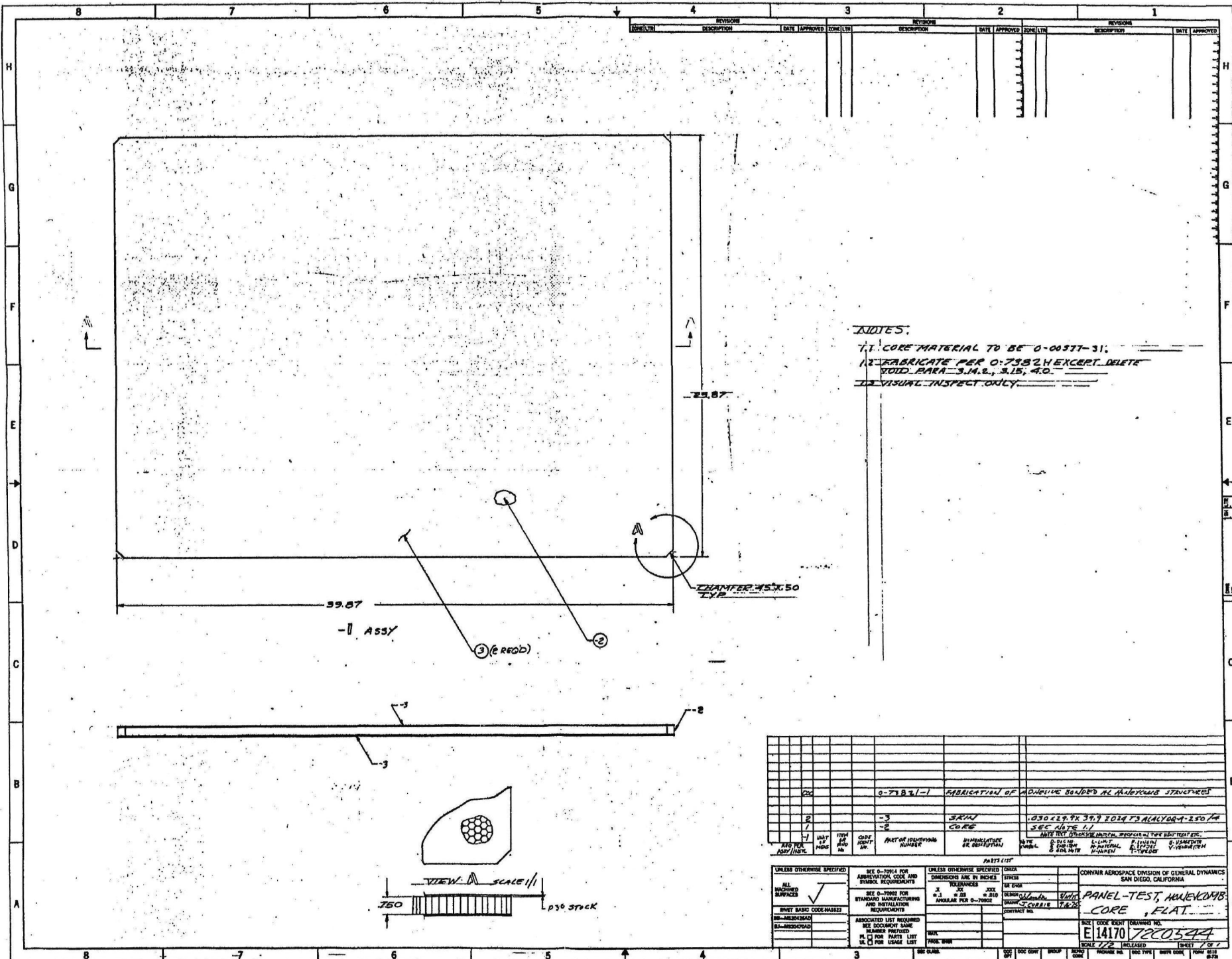
Dwg. No. 72C0546; Panel-Test, Bonded, Stiffened

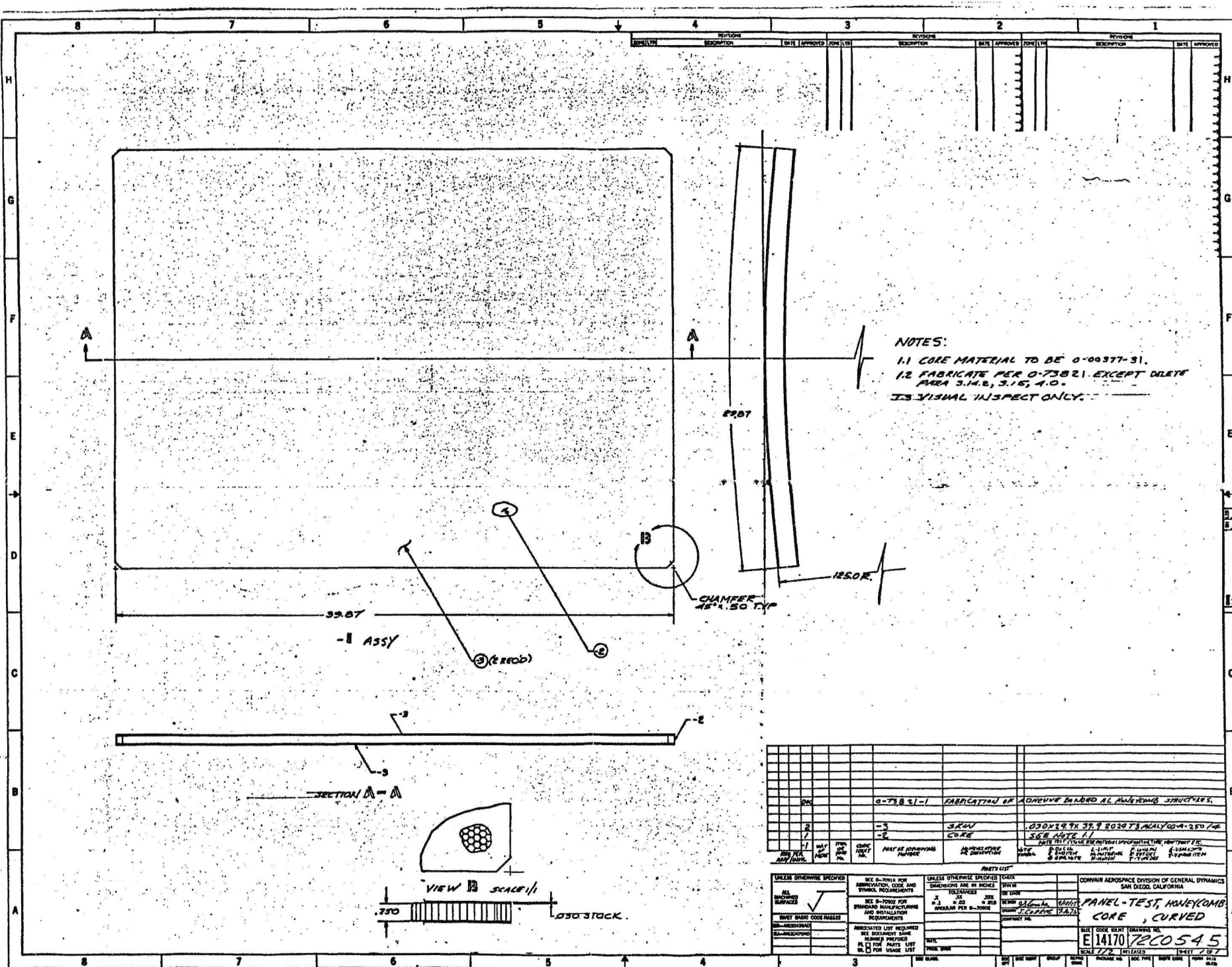
Dwg. No. 72C0547; Panel-Test, Bonded, Stiffened, Curved

**"Page missing from available version"**

page 42

Pgs 43  
45  
47  
49 } foldouts





720545







## APPENDIX C

### VIBRATION TEST INSTRUMENTATION AND PROCEDURES

Instrumentation used in this program, for both vibration and acoustic tests, is shown in Table 1A.

Vibration resonance testing was accomplished on all but Panel a of the seven test panels. Panel a, Appendix A, was not vibration tested for the following reason. It was originally configured as Panel a.1. After it was vibration tested and acoustic transmission loss data had been obtained, the panel was returned to the factory where the graphite/epoxy strips were removed from the aluminum frames. The panel was then returned directly to the Acoustics Laboratory for additional TL tests, since it was not feasible to re-run vibration tests.

For the vibration tests, each panel was mounted in a frame which provided the same edge restraints as would be obtained during the subsequent acoustic tests. The frame (including panel), was installed on an electrodynamic shaker so that the panel was subjected to inertial excitation, as shown in Figure 1A. Edge restraints for both vibration and acoustic tests were essentially as shown in Figure 2A. Each panel was subjected to a 0.25 grms sinusoidal vibration sweep from 20 to 1000 Hz at a rate of 2 min/octave.

Accelerometers, as noted in Table 1A, suitably disposed on each test panel and frame, as shown in Figure 3A, plus roving accelerometers, were used to determine resonant frequencies and modes of vibration. All accelerometer data were recorded on a strip chart recorder (Table 1A). Resonant frequencies were obtained from amplitude maxima; modes were determined by observation of phase relationships among the trasducers; and panel damping was obtained from the one-half power point bandwidths. Data are contained in Table 2A.

**Page Intentionally Left Blank**

## APPENDIX D

### ACOUSTIC TEST CHAMBERS - INSTRUMENTATION AND PROCEDURES

#### Acoustic Test Chambers

The general arrangement of the reverberation and anechoic rooms of the General Dynamics Acoustic Test Laboratory is shown in Figure 4A. The volume of the reverberant room is approximately  $56.63 \text{ m}^3$ , and the average absorption coefficient is about 0.02 (References 10 and 11). Nominal dimensions of the room are; length = 4.88 m, width = 3.96 m, and height = 3.05 m. Using these dimensions, acoustic modes of the room were calculated to be as follows:

$$f_{lwh} = \frac{c}{2} \left[ \frac{1}{l^2} + \frac{1}{w^2} + \frac{1}{h^2} \right]^{1/2}$$

where  $c$  is the speed of sound

$$f_{111} = 80 \text{ Hz}$$

$$f_{221} = 125 \text{ Hz}$$

$$f_{222} = 160 \text{ Hz}$$

$$f_{442} = 250 \text{ Hz}$$

$$f_{444} = 315 \text{ Hz}$$

$$f_{884} = 500 \text{ Hz}$$

$$f_{888} = 630 \text{ Hz}$$

etc.

The existence of these modes was confirmed experimentally by tests reported in Reference 14. It is noted that only three dimensional modes of the room were significant, linear modes were suppressed because of the corner locations of the loudspeakers as shown in Figure 4A.

Significant modes of the anechoic room were found at 84, 115, 144, 206, etc., Hz. The influence of the room acoustic modes on the panel test data are discussed in the main body of the report.

## Instrumentation

Instrumentation used in the acoustic surveys of the test chambers (and test panels) is shown in Figure 5A. The various fixed microphone positions, in addition to the use of "roving" microphones, are shown in Figure 6A. It is noted that during the room modal surveys, the test panel window was occupied by a solid, 0.25 inch aluminum plate which was backed and was heavily damped by compressed fiber-glass blankets. The purpose of the heavy, damped plate was to assure that acoustic modes which were excited in one room would not couple significantly with modes in the adjacent room.

The purpose of the room surveys was twofold; first, to determine the room modes and frequencies in order that their effects could be removed from test panel transmission loss data and; second, to find microphone locations for the actual panel transmission loss tests which would assure uniform pressure distributions across the panels. Roving microphones were used for determination of room modes, while both roving and fixed microphones were used to establish optimum positions for the panel transmission loss tests.

The following fixed microphone positions were finally selected for the transmission loss tests on the contract panels:

Reverberation Room - On panel centerline at a distance of 0.90 m.  
from panel.

Anechoic Room - On panel centerline at a distance of 0.25 m  
from panel.

## Test Procedures

Random noise generated in the reverberation room, Reference Figure 5A, was on an octave band basis. Only the center one-third octave band of noise, however, was used for obtaining transmission loss data. This procedure eliminated any effects of filter roll-off on the generated noise and tended to minimize any



synergistic effects which could result from the occurrence of an acoustic or structural resonance at the extreme edge of a filter bandwidth.

All test panels were installed, in sequence, in the window between the reverberation and anechoic rooms, as shown in Figures 4A, 6A, 7A and 8A. Before any transmission data were obtained on a panel, a check was made for acoustic "leaks" around the panel while an octave band of noise centered at 5000 Hz was being generated in the reverberation room. Each panel was then subjected to octave bands of noise, with the center one-third octaves being used for data purposes. Center frequencies from 31.5 to 8000 Hz were covered in succession. At the conclusion of a "run" on a panel, microphones were interchanged between the reverberation and anechoic rooms, and the "run" was repeated. This obviated the requirement for separate microphone calibrations and accounted for any uncertainty related to changes in microphone sensitivity.

The data obtained during the procedures described above were "noise reduction" and not "transmission loss" data. Transmission loss is defined as the ratio (expressed in decibels) of the acoustic energy transmitted through a panel to the acoustic energy incident upon it (Reference 10). That is, transmission loss (TL) is related only to the panel. Noise reduction (NR), however, is the difference in sound pressure levels on the two sides of a panel where the primary side is in a reverberant field and the microphone on the secondary side is near the panel surface. It is obvious that the acoustic properties of the secondary enclosure, i.e., anechoic room, are directly involved in the obtained panel data.

Transmission loss can be described by the equation  $TL = NR + K$ , where K is a lumped constant. The constant K will vary with frequency, directivity factor, and to some extent with the properties of the panel under test. Selection of the microphone positions for the test program was aimed at minimizing secondary variables. The constant, K, was determined by first having a "standard" panel

tested in a qualified outside laboratory to obtain its transmission loss properties, viz, the Riverbank Acoustics Laboratories of the Armour Research Foundation; the standard panel was 0.10 inch thick, alclad 2024-T3 aluminum alloy. The same panel was then re-tested in the General Dynamics Acoustics Laboratory and the differences between the noise reduction data (General Dynamics) and the transmission loss data (Riverbank) were obtained as "K" vs frequency. These results, obtained in 1958, were reported in Reference 15. Before tests on the contract panels were initiated, the standard panel was re-tested. This was done to assure that there had been no change in the test chamber properties over the years, but primarily to assure the competence of the test personnel. The results of these tests are shown in Figure 9A; the lumped constant, K, is shown in Figure 10A.

Table 1A. Test Facilities and Instrumentation

The test facilities and equipment used during the performance of this test are listed below.

TYPE	MANUFACTURER	MODEL	S/N	RANGE	ACCURACY	Calibration Interval
Vibration Sys. No. 4	M. B.	C-200	202	5 Hz-3K Hz	Controlled	-
Charge Amplifiers	Endevco	2713	MA95	2 Hz-20K Hz	±5%	9 Months
Charge Amplifiers	Endevco	2713	YB19	2 Hz-20K Hz	±5%	9 Months
Charge Amplifiers	Endevco	2713	MA93	2 Hz-20K Hz	±5%	9 Months
Charge Amplifiers	Endevco	2713	LC41	2 Hz-20K Hz	±5%	9 Months
Charge Amplifiers	Endevco	2713	RB55	2 Hz-20K Hz	±5%	9 Months
Charge Amplifiers	Endevco	2713	MA94	2 Hz-20K Hz	±5%	9 Months
Accelerometers	Endevco	2226	NC86	2 Hz-5K Hz	±5%	Daily
Accelerometers	Endevco	2226	NB35	2 Hz-5K Hz	±5%	Daily
Accelerometers	Endevco	2226	WQ11	2 Hz-5K Hz	±5%	Daily
Accelerometers	Endevco	2226	WQ05	2 Hz-5K Hz	±5%	Daily
Accelerometers	Endevco	2226	SB90	2 Hz-5K Hz	±5%	Daily
Accelerometers	Endevco	2226	MD33	2 Hz-5K Hz	±5%	Daily
Recorder, Strip	Hewlett-Packard	7700	240409818	5 Hz-100K Hz	±1 dB	6 Months
Vibration Fixture	Convair	833-1	-	-	-	-
Noise Generator	General Radio	1390B	3245	5 Hz-20K Hz	±1 dB	6 Months
Multifilter	General Radio	1925	2726	25 Hz-20K Hz	±1 dB	-
Amplifier	McIntosh	MI-200A	1074	200 Watts	-	-
Speaker	Altec Lansing	604C	-	-	-	-
Microphone	Altec	21BR-150	10764	5-11K Hz	±1 dB	Daily
Microphone	Altec	21BR-150	10486	5-11K Hz	±1 dB	Daily
Analyzer	Spectral Dynamics	201	17	10 Hz-20K Hz	±2%	6 Months

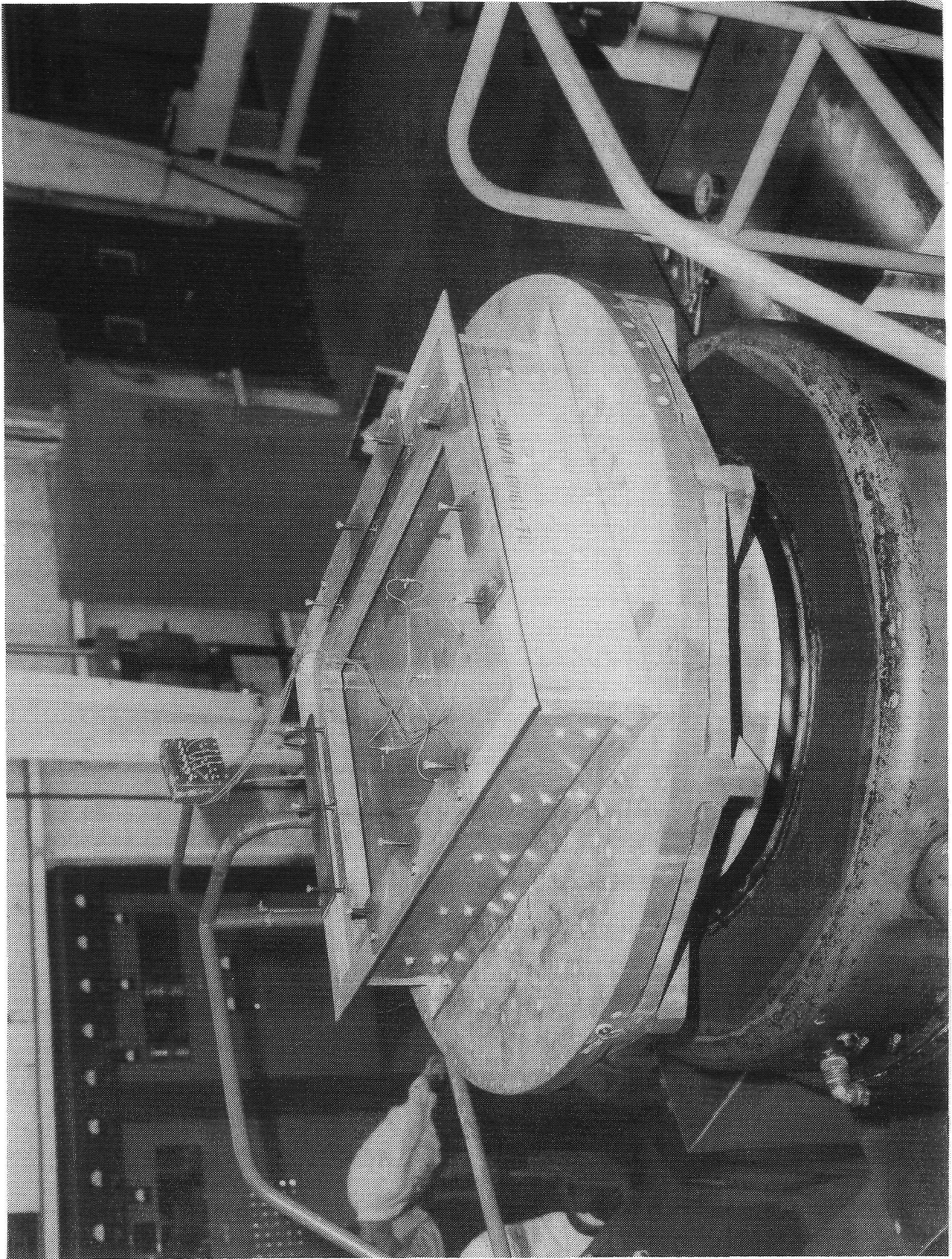


Figure 1A. Vibration Test Setup

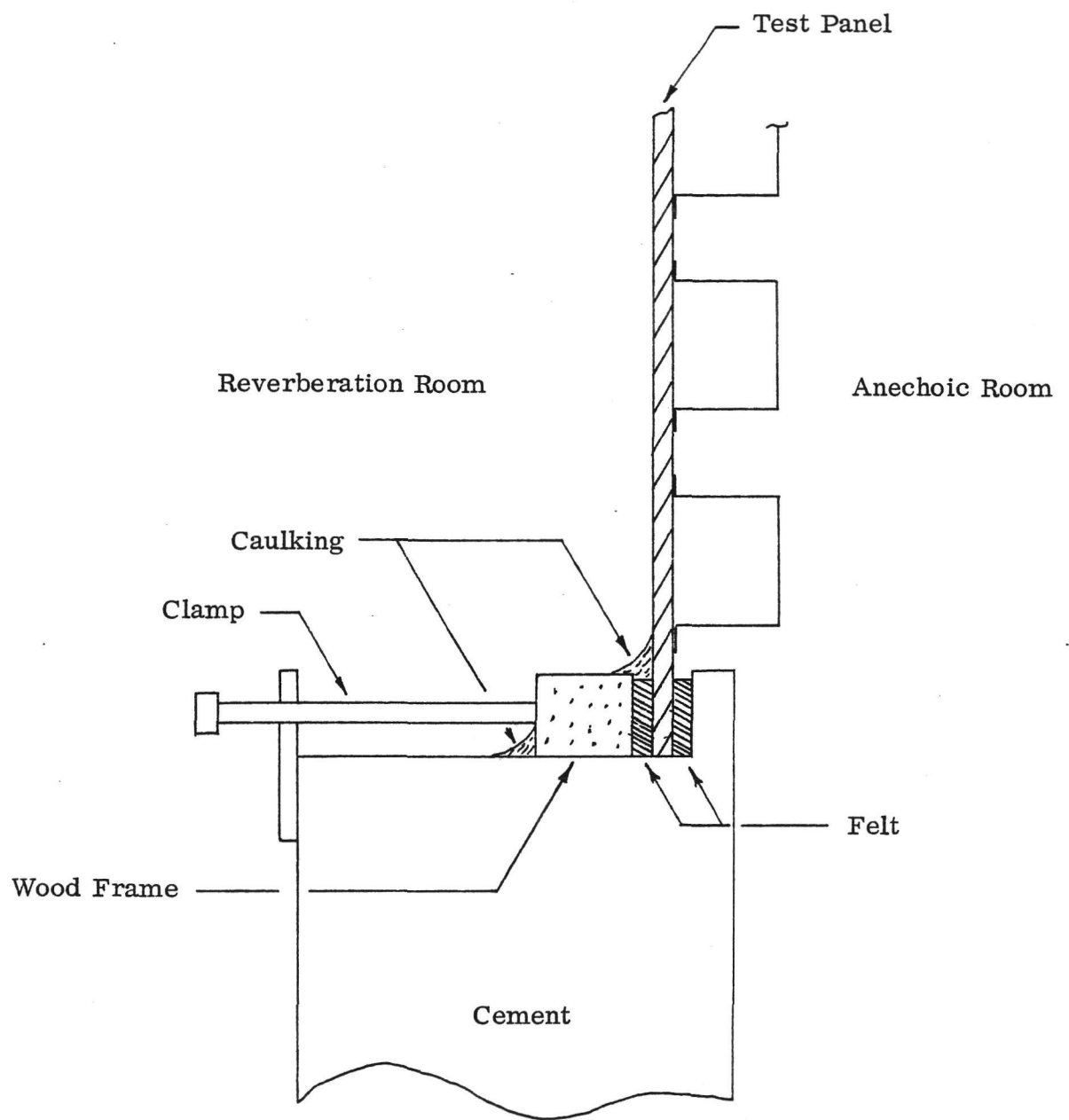


Figure 2A. Acoustic Test Setup

Table 2A. Summation of Vibration Data

Panel	Freq. (Hz)	Transmission Factor (Response To Input Accelerometer)					Damp- ing Ratio c/cc
		#2	#3	#4	#5	#6	
a. 1 (Between Frames)	500	+12.1	37.9	+11.7	+11.0	+8.6	0.020
	240	+1.4	8.3	+2.6	+8.3	+6.2	
b	800	+8.9	25.0	+6.1	+35.7	+34.6	0.018
e	225	+12.0	20.0	+15.2	+10.7	+10.0	0.040
f (Unsupported)	450	-12.8	2.4	+10.0	-1.6	+2.2	0.022
f (Supported)	430	-9.0	2.6	+7.3	-2.7	+2.7	0.022
c	825	+5.7	21.7	+5.4	+17.4	+16.0	0.005
d	470	+5.0	7.9	+5.4	+7.5	+3.4	0.013

Note: (+) Indicates In-phase With Center (#3) Response Accel.

(-) Indicates Out-Of-Phase With Center (#3) Response Accel.



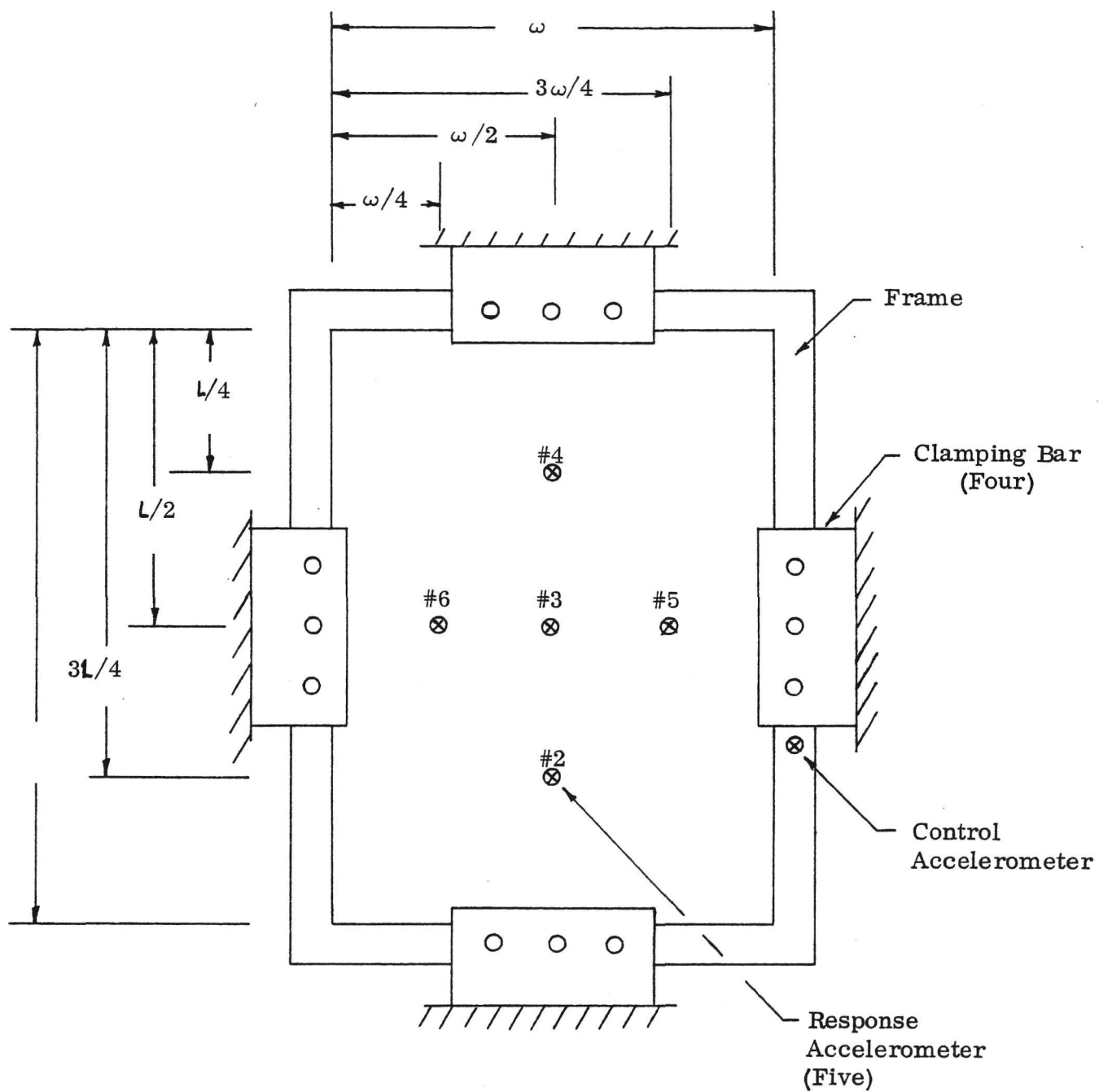


Figure 3A. Vibration Test Setup

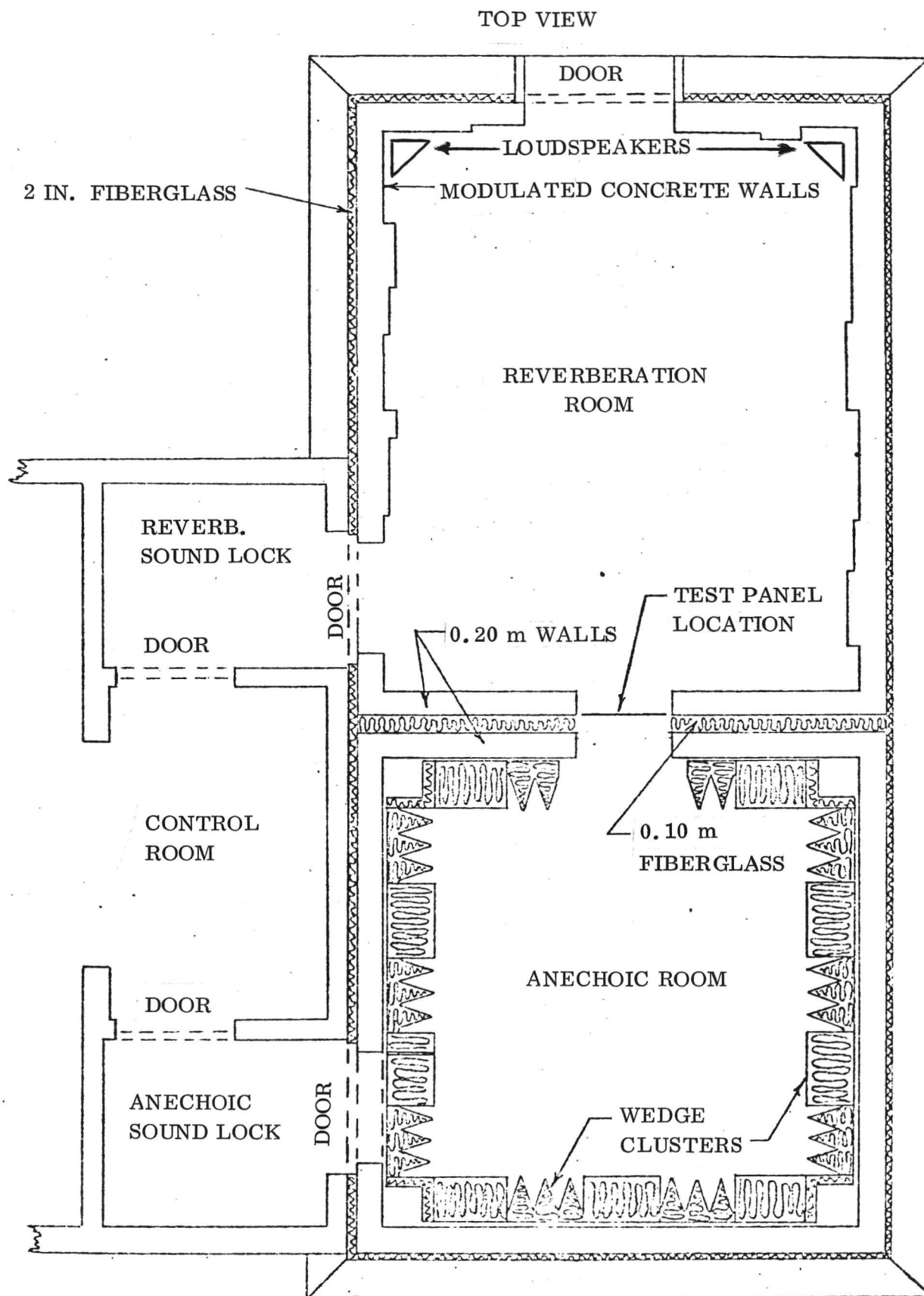


Figure 4A. Anechoic and Reverberation Rooms

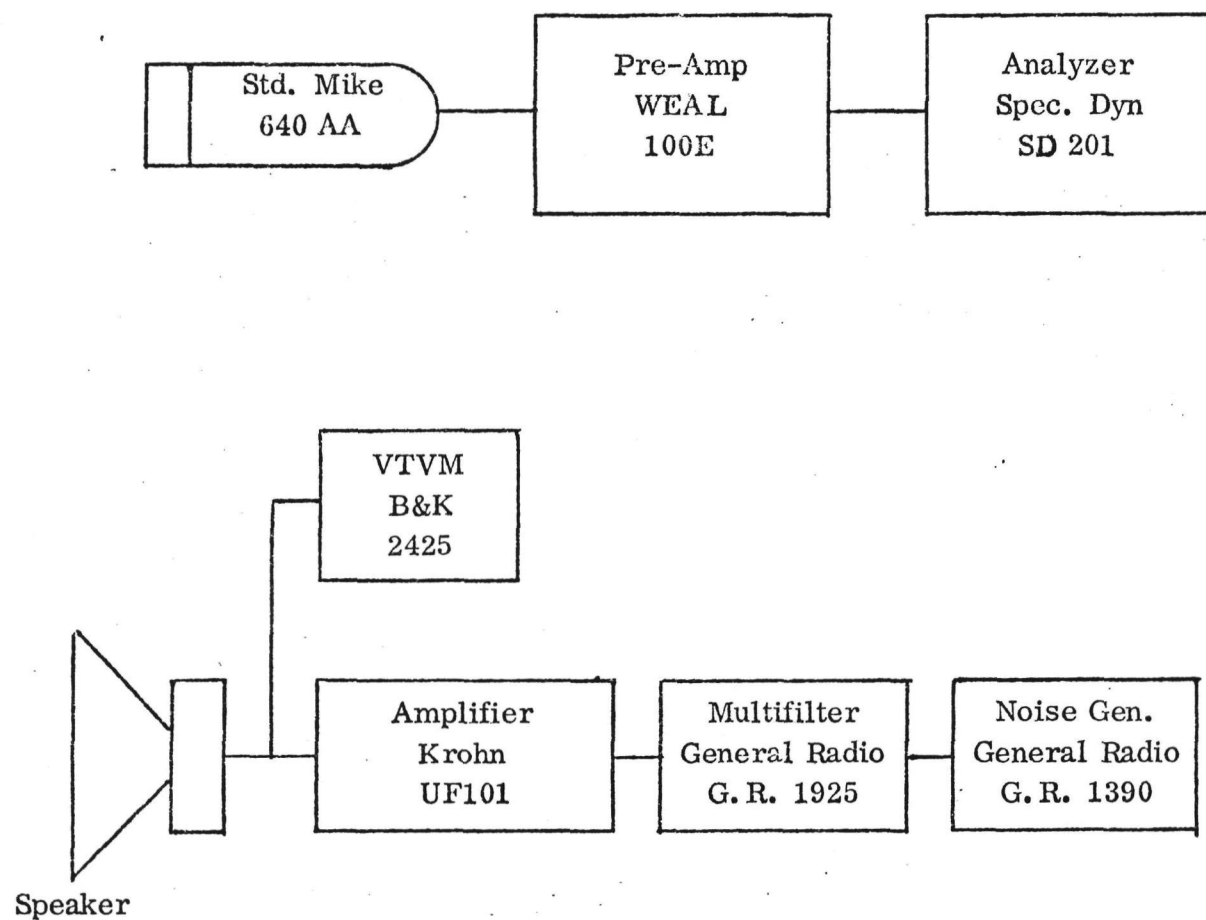


Figure 5A. Instrumentation

Note: Dimensions are in inches. To convert to metres, multiply by .025.

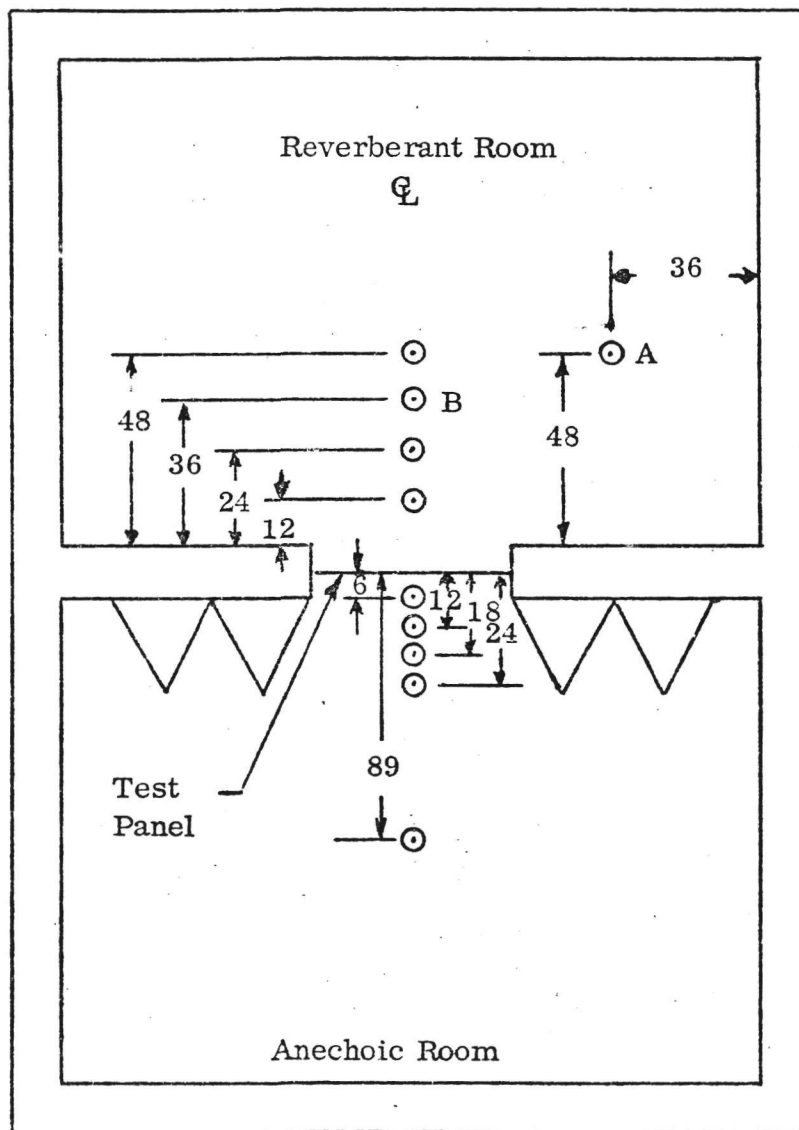


Figure 6A. Microphone Positions  
(not to scale)

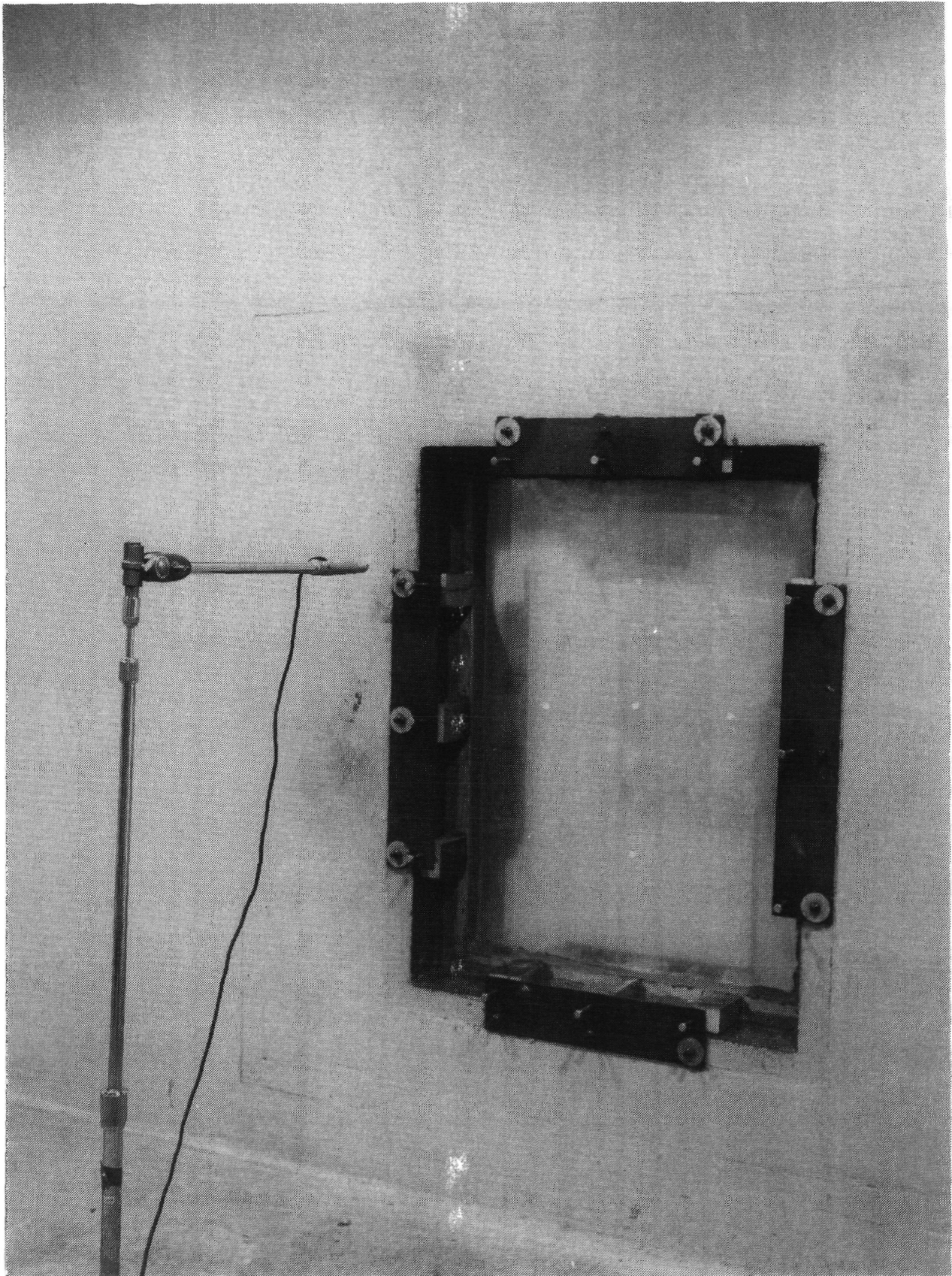


Figure 7A. Acoustic Test Setup (Reverberation Room Side)



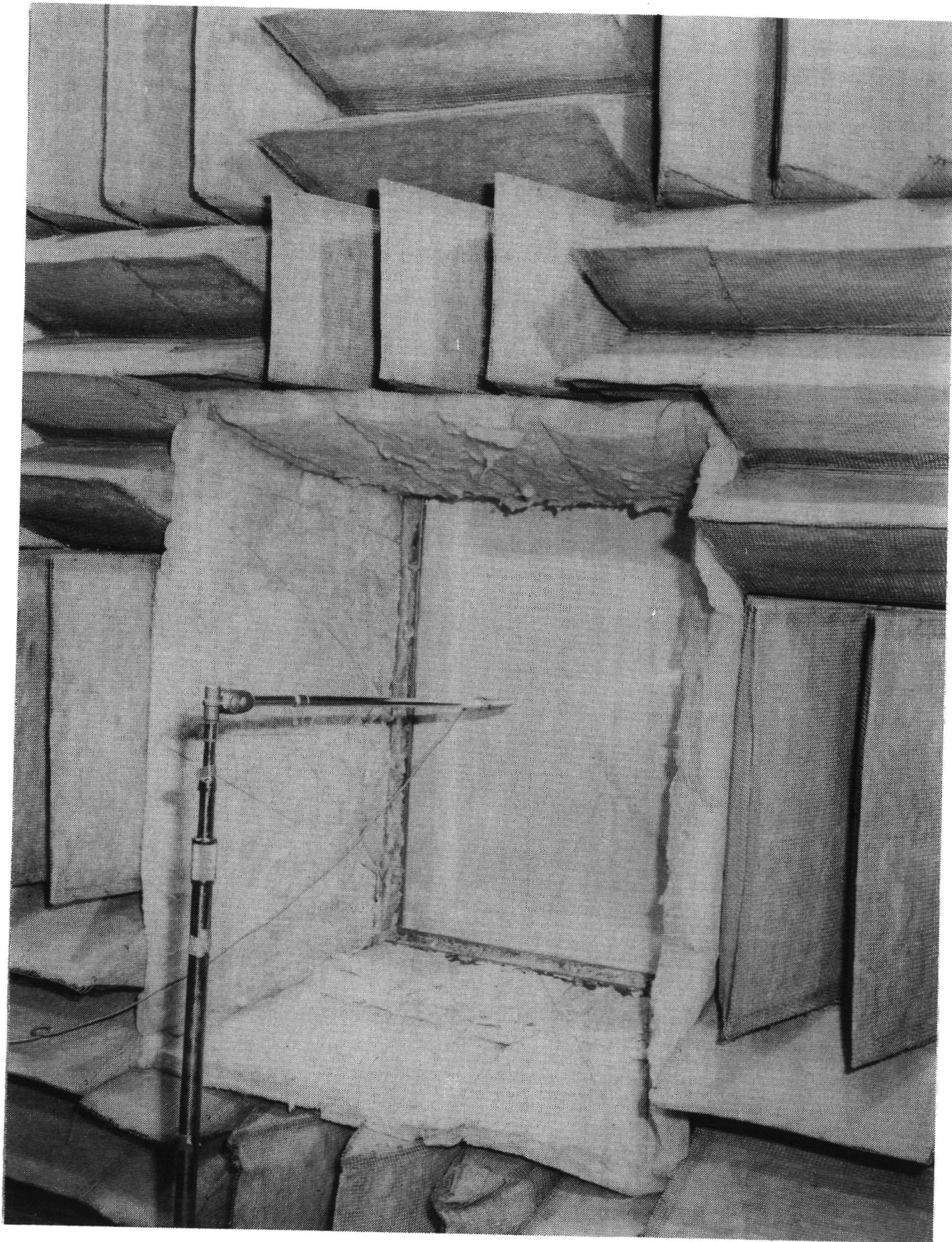


Figure 8A. Acoustic Test Setup (Anechoic Room Side)



ADD 4.9 DB TO OBTAIN OCTAVE BAND LEVEL

THIRD-OCTAVE BAND TRANSMISSION LOSS - dB

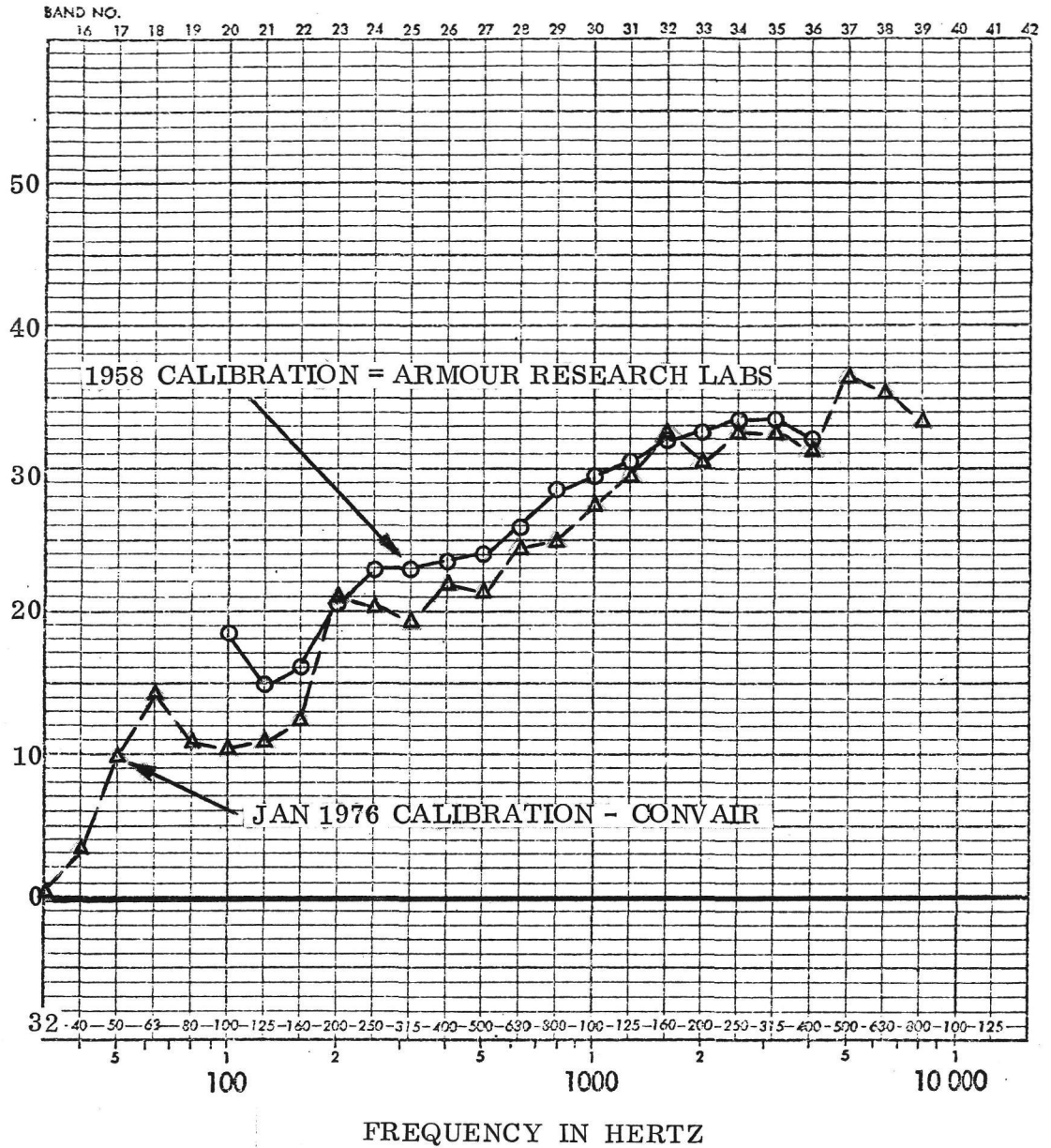


Figure 9A. Standard Panel (0.10 In. Flat Sheet Al Alloy)  
Transmission Loss Calibration





ADD 4.9 DB TO OBTAIN OCTAVE BAND LEVEL

LUMPED CONSTANT, K, FOR CALCULATION OF  
THIRD-OCTAVE BAND TRANSMISSION LOSS - dB

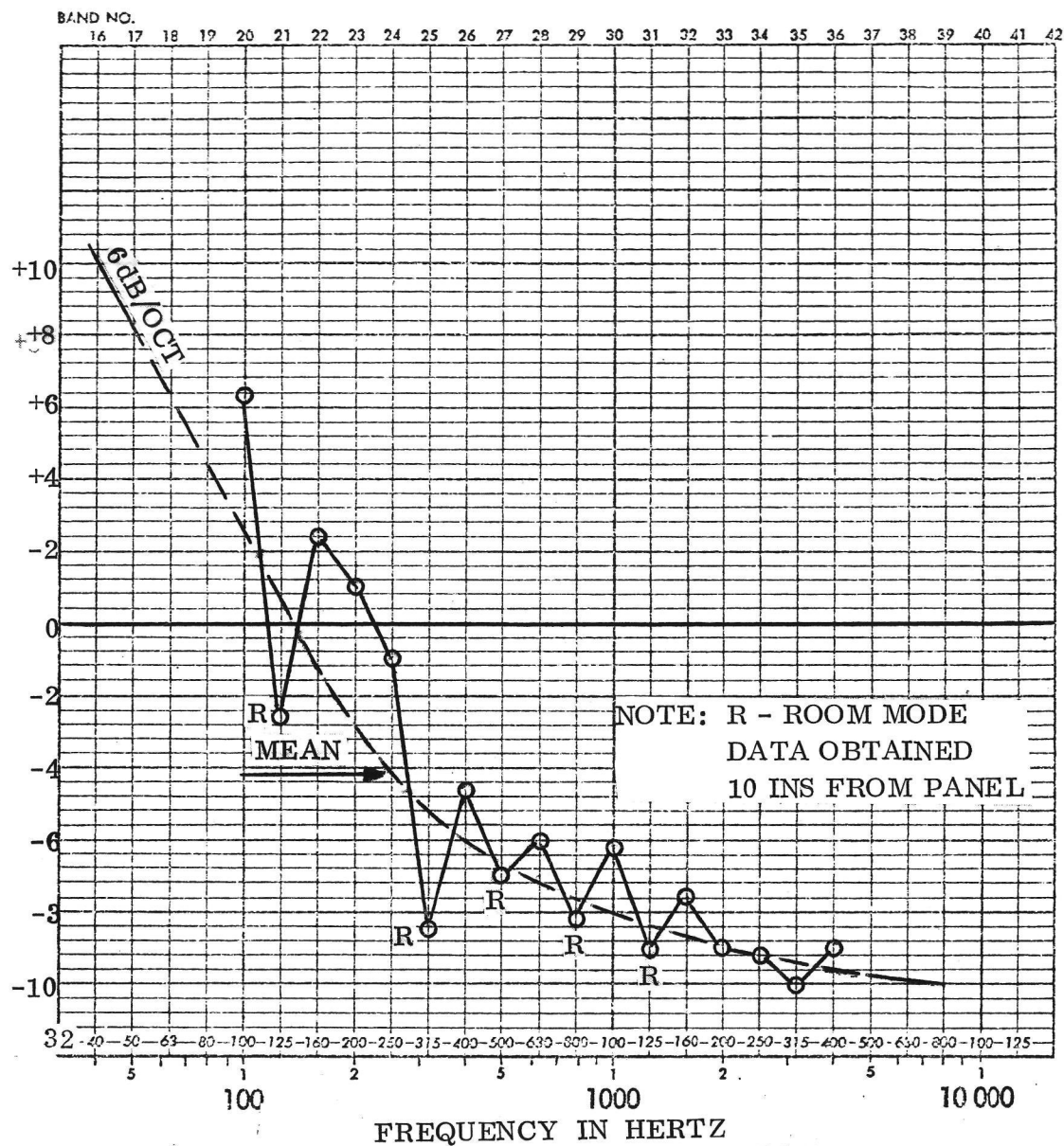


Figure 10A. Lumped Constant K Equals All Room and Panel Constants  
 $K = (\text{Transmission Loss}) - (\text{Noise Reduction})$  or  $TL = NR + (K)$

1. Report No. NASA CR-145104		2. Government Accession No.		3. Recipient's Catalog No.	
4. Title and Subtitle  Low-Frequency Noise Reduction of Lightweight Airframe Structures				5. Report Date August 1976	
				6. Performing Organization Code	
7. Author(s)  G. L. Getline				8. Performing Organization Report No. CASD-NAS-76-032	
				10. Work Unit No.	
9. Performing Organization Name and Address  General Dynamics Convair Division P.O. Box 80847, San Diego, CA 92138				11. Contract or Grant No. NAS1-13910	
				13. Type of Report and Period Covered Technical June 1975-Aug 1976	
12. Sponsoring Agency Name and Address  National Aeronautics and Space Administration Langley Research Center Hampton, VA 23665				14. Sponsoring Agency Code	
15. Supplementary Notes					
16. Abstract  This report presents the results of an experimental study to determine the noise attenuation characteristics of aircraft-type fuselage structural panels constructed so as to provide a high stiffness to weight ratio. Of particular interest was noise attenuation at low frequencies, below the fundamental resonances of the panels. All panels were flightweight structures for transport type aircraft in the 34 050 to 45 400 kg (75,000 to 100,000 pounds) gross weight range. Test data include the results of vibration and acoustic transmission loss tests on seven types of isotropic and orthotropically stiffened, flat and curved panels. The results of the study show that stiffness controlled-acoustically integrated structures can provide very high noise reductions at low frequencies without significantly affecting their high frequency noise reduction capabilities.					
17. Key Words (Suggested by Author(s)) Low Frequency Noise Transmission Loss Noise Reduction Stiffness Control Composite Structures			18. Distribution Statement  Unlimited		
19. Security Classif. (of this report) Unclassified		20. Security Classif. (of this page) Unclassified		21. No. of Pages 61	
22. Price*					

\* For sale by the National Technical Information Service, Springfield, Virginia 22161